

4. EXPLANATORY NOTES¹

Shipboard Scientific Party²

EXPLANATORY NOTES

Standard procedures for both drilling operation and preliminary shipboard analysis of the material recovered have been regularly amended and upgraded since 1968 during Deep Sea Drilling Project and Ocean Drilling Program drilling. In this chapter, we have assembled information to help the reader understand the basis for our preliminary conclusions and to help the interested investigator select samples for further analysis. This information regards only shipboard operations and analyses described in the site reports in the *Initial Reports*, or Part A, of the Leg 107 *Proceedings of the Ocean Drilling Program*. Methods used by various investigators for further shore-based analysis of Leg 107 data will be detailed in the individual scientific contributions published in the *Final Report*, or Part B, of the volume.

AUTHORSHIP OF SITE REPORTS

Authorship of the site reports is shared among the entire shipboard scientific party, although the two co-chief scientists and the staff scientist edited the material prepared by other individuals. The site chapters are organized as follows (authorship in parentheses):

Site Summary (Auroux, Kastens, Mascle, J.)
Background and Objectives (Kastens, Mascle, J.)
Operations (Huey, Kastens, Mascle, J.)

¹ Kastens, K. A., Mascle, J., Auroux, C., et al., 1987. *Proc. Init. Repts. (Pt. A)*, ODP, 107.

² Kim A. Kastens (Co-Chief Scientist), Lamont-Doherty Geological Observatory, Palisades, NY 10964; Jean Mascle (Co-Chief Scientist), Laboratoire de Géodynamique Sous-Marine, Université Pierre et Marie Curie, BP 48, 06230 Villefranche-sur-Mer, France; Christian Auroux, Staff Scientist, Ocean Drilling Program, Texas A&M University, College Station, TX 77843; Enrico Bonatti, Lamont-Doherty Geological Observatory, Palisades, NY 10964; Cristina Broglia, Lamont-Doherty Geological Observatory, Palisades, NY 10964; James Channell, Department of Geology, 1112 Turlington Hall, University of Florida, Gainesville, FL 32611; Pietro Curzi, Istituto di Geologia Marina, Via Zamboni, 65, 40127 Bologna, Italy; Kay-Christian Emeis, Ocean Drilling Program, Texas A&M University, College Station, TX 77843; Georgette Glaçon, Laboratoire de Stratigraphie et de Paléocéologie, Centre Saint-Charles, Université de Provence, 3, Place Victor Hugo, 13331 Marseille Cedex, France; Shiro Hasegawa, Institute of Geology, Faculty of Science, Tohoku University, Aobayama, Sendai, 980, Japan; Werner Hieke, Lehrstuhl für Allgemeine, Angewandte und Ingenieur-Geologie, Abt. Sedimentforschung und Meeresgeologie, Technische Universität München, Lichtenbergstrasse 4, D-8046 Garching, Federal Republic of Germany; Floyd McCoy, Lamont-Doherty Geological Observatory, Palisades, NY 10964; Judith McKenzie, Department of Geology, University of Florida, 1112 Turlington Hall, Gainesville, FL 32611; Georges Mascle, Institut Dolomieu, Université Scientifique et Médicale de Grenoble, 15 Rue Maurice Gignoux, 38031 Grenoble Cedex, France; James Mendelson, Earth Resources Laboratory E34-366, Department of Earth, Atmospheric and Planetary Sciences, Massachusetts Institute of Technology, 42 Carleton Street, Cambridge, MA 02142; Carla Müller, Geol. Paläont. Institut, Universität Frankfurt/Main, 32-34 Senckenberg-Anlage, D-6000 Frankfurt/Main 1, Federal Republic of Germany (current address: 1 Rue Martignon, 92500 Rueil-Malmaison, France); Jean-Pierre Réhault, Laboratoire de Géodynamique Sous-Marine, Université Pierre et Marie Curie, BP 48, 06230 Villefranche-sur-Mer, France; Alastair Robertson, U.S. Geological Survey, 345 Middlefield Road, Menlo Park, CA 94025 (current address: Department of Geology, Grant Institute, University of Edinburgh, Edinburgh, EH9 3JW, United Kingdom); Renzo Sartori, Istituto di Geologia Marina, Via Zamboni, 65, 40127 Bologna, Italy; Rodolfo Sprovieri, Istituto di Geologia, Corso Tukory, 131, Palermo, Italy; Masayuki Torii, Department of Geology and Mineralogy, Faculty of Science, Kyoto University, Kyoto, 606, Japan.

Lithostratigraphy (Hieke, Mascle, G., McCoy, McKenzie, Réhault, Robertson, Sartori)
Igneous Petrology (Bonatti)
Biostratigraphy (Glaçon, Hasegawa, Müller, Sprovieri)
Paleomagnetism (Channell, Torii)
Organic and Inorganic Geochemistry (Emeis)
Physical Properties (Auroux, Curzi)
Downhole Measurements (Broglia, Mendelson, Réhault)
Seismic Stratigraphy (Auroux, Mascle, J., Mendelson)
Summary and Conclusions (Kastens, Mascle, J.)

Following the text in each site chapter are summary graphic lithologic and biostratigraphic figures, core descriptions ("barrel sheets"), and photographs of each core.

SITE APPROACH AND SITE SURVEY

Most site approaches were laid out to follow the track of existing high-quality seismic reflection profiles. Typically, seismic gear was streamed 10–15 nmi in advance of the first pass over the beacon drop position. The agreement between the old and new reflection profiles and bathymetric profiles was then carefully monitored during the site approach. At sites where positioning was not critical, and old and new profiles agreed well, the dynamic positioning beacon was dropped on the first pass. In cases where the target was small (sites 651, 652, and 654), a seismic line was run across the drop point to verify the geologic setting of the drop point and to calibrate the *JOIDES Resolution's* single channel data vs. the multichannel data from which the approved location had been chosen. The ship then made a Williamson turn to the reciprocal course, and the beacon was dropped on the second (or in one case the third) pass across the site. The choice of the exact moment to drop the beacon was based on the real-time seismic reflection and bathymetric profiles.

During transits between sites and site approaches, bathymetric data were collected at 3.5 and 12 kHz. The standard 3.5-kHz system uses an array of 12 Raytheon TR-109 transducers and a Raytheon PTR-105B transceiver. The 3.5-kHz profiles were displayed on an EDO 550 flatbed recorder. A Raytheon CESP-III correlator was used to improve signal-to-noise ratio. The correlator introduced a systematic error in apparent depth. The magnitude of the error depends on pulse width; at the 100-ms pulse width that was used throughout Leg 107, the water depth as read on the recorder was 75 m too deep. An experimental towed 3.5-kHz transducer array, designed for high-speed (as fast as 13 kt) towing, was tested on some site approaches. The towed fish utilizes four in-line Raytheon TR-109 transducers. Pulse width for the towed fish, as for the hull-mounted array, was 100 ms. The transducer array was towed at a depth of about 10 m; in contrast the hull-mounted transducer was 6 m below sea level.

The ship has two 12-kHz transducers: a Raytheon TR-12/34 is mounted aft of the moonpool and an EDO 323B is mounted forward, under the bridge. During Leg 107, the EDO was more commonly used on site approaches because the aft transducer is in a noisier location. The 12-kHz system uses an EDO 248C transceiver and an EDO 550 flatbed recorder. The 12-kHz system has no correlator so water depths can be read accurately.

Water depths reported as "PDR (precision depth records) uncorrected depths" were read from this 12-kHz record, assuming 1500-m/s sound velocity. Water depths reported as "PDR corrected water depths" have been further corrected for the sound velocity according to the tables of Matthews (1939). Depths reported as "DPM" (drill pipe measure) are based on the sum of the measured lengths of the drill pipe components which were in the water at the time that the seafloor was felt by the weight-on-bit indicator. Depths reported relative to the rig floor can be converted into depths below sea level by subtracting 10.5 m, which was the height of the dual elevator stand on the rig floor above sea level during Leg 107.

During site approaches, single channel seismic reflection data were collected beginning 10–15 nmi before the first crossing of the beacon drop point. The sound source consisted of two synchronized 80-in.³ Seismic Systems Inc. water guns. The streamer is a Teledyne 178. The active section, 100 m long, was towed 500 m behind the ship. The active section contains 60 equally spaced hydrophones whose output is transformer-coupled to the ship. The signal was amplified and displayed on two analog monitor records at chooseable band-widths in real time; these displays each use an EDO 550 recorder. In addition, the signal was digitized by a Masscomp 561 computer and displayed as a processed record on a Printronix high-resolution graphic printer, approximately 3 min after real time. The unprocessed digital signal was also recorded on 9-track magnetic tape using an SEG-Y format and a density of 1600 bits/in. The header file for each shotpoint on the magnetic tape includes the following information: shotpoint number, date and time, wind speed, wind direction, ship's speed (pit log), ship's gyroscope heading, cumulative distance traveled, streamer and gun depth, and information concerning timing of gun firing. All geophysical survey data collected during Leg 107 are presented in the "Underway Geophysics" chapter (this volume).

A variety of navigational aids was used during Leg 107 site approaches. The ship has two transit satellite receivers: a Magnavox 1107-GPS, located in the underway geophysics lab, and a Magnavox 702A-3 located on the bridge. About 1 fix out of 20 was received by one receiver and not the other, with the 1107-GPS receiving more often. The satellite receiver in the underway geophysics lab receives fixes from the Global Positioning System (GPS) as well as the standard transit satellite system. During Leg 107, GPS fixes were received during two time windows each day: one window 2–3 hr long around midday and a second window 4–5 hr long in the mid- to late evening to earliest morning. On Leg 107 local (ship's) time was equal to Greenwich Mean Time. The official site positions reported at the beginning of each site chapter are based on an average of GPS and transit satellite fixes received while on station.

The entire cruise was within the area covered by the 7990 Loran-C chain. However, Loran positioning, using the ship's Si-Tex/Koden 757 Loran receiver, proved to be highly erratic and dependent on time of day, ship's heading, and atmospheric conditions. Loran position and the time delays for each master/slave Loran pair are reported in the Operations summary for each site.

When neither GPS nor Loran continuous fixes were available, the ship was navigated by transit satellites and dead reckoning. Inputs to the dead reckoning calculations come automatically from the ship's gyroscope and a Ben Co. Super Galathea electromagnetic pit log; alternatively speed and course can be entered manually. Both the Magnavox 1107-GPS and the Magnavox 702HP satellite receivers calculate dead reckoning positions.

After the beacon was dropped, the ship returned to the beacon to begin dynamic positioning. In some cases, the drill site was as far as 400 m away from the beacon, either to allow for flexibility in siting a second hole at the same beacon, or to make

up for slight errors in beacon drop position. The hole locations marked on the seismic reflection profiles illustrated in each site chapter take into account both the 500-m offset between streamer position and ship position at the time of the beacon drop, and also the offset, if any, between beacon position and drill site.

DRILLING CHARACTERISTICS

Drilling and Coring Techniques

Three different drilling/coring tools were used during Leg 107. The Advanced Piston Corer (APC) combines the principles of oceanographic piston coring and stored energy in the drill string to produce relatively undisturbed cores at very high recovery rates. It utilizes the technology of the past DSDP Hydraulic Piston Corers (DSDP, 1983, 1984) while incorporating a simplified seal system which results in a piston corer capable of 76% greater coring force (as much as 28,000 lbf). The core bit used for APC coring has a throat large enough to allow the piston corer to be hydraulically extended beyond the bit. In the piston coring operation the corer is locked together by shear pins until it has been lowered into place at the bit by the sand line. Upon landing the seals of the corer seal off the bore of the drill string. Hydraulic pressure is then applied to the drill pipe with the rig pumps until forces resulting from differential pressure cause the shear pins to fail. The inner core barrel is thus forcibly ejected through the bit while moving past a fixed internal piston. The extended assembly and the full inner barrel are then recovered with the sand line. Then, the pipe is advanced by the length of the next joint of drill pipe to be added to the drill string.

A magnetic orientation system can be used to determine the orientation of cores taken by the APC with respect to magnetic north. The system consists of an Eastman Magnetic Multishot Survey Instrument. The Eastman Multishot and the double reference line on the core liner are aligned together. An anti-spiral system prevents rotation of the corer telescoping section relative to the piston rod section.

The Extended Core Barrel (XCB) coring system is a rotary system similar in many ways to the Rotary Core Barrel system (see below). It uses the same core catchers and butyrate core liner. The XCB is a free-falled core barrel which latches in place in the outer core barrel and rotates with the outer barrel. The XCB can be deployed in the same Bottom Hole Assembly (BHA) as the APC. The XCB core barrel has a cutting shoe rotating with the roller cone bit. This cutting shoe can extend 7 in. beyond the face of the core bit and retracts automatically into the core barrel to a position above the roller cones when hard material is drilled. In the extended position the cutting shoe shields the incoming core from disturbance caused by the bit jet hydraulics.

The Rotary Core Barrel (RCB) was used for routine coring in medium to hard formations. This tool is a modified Hycalog wireline core barrel. This design uses a drill collar as the outer barrel. These collars are the same as those used elsewhere in the BHA. The core barrel can remain motionless relative to the incoming core while the bit and the outer core barrel rotate. Cores are cut by rotating and lowering of the entire drill string. The cutters of the core bit and the circulation of seawater remove rock or sediment ahead of the bit but leave a central stub that becomes the core.

Drilling Parameters

Because water circulation down the hole is open, cuttings are lost onto the seafloor and cannot be examined. However, in uncored or unrecovered intervals, it is sometimes possible to deduce some information about sedimentary stratification from an examination of the behavior of the drill string as observed and recorded at the rig floor. Generally, the harder the layer, the

slower it is to penetrate; for this reason, graphs of drilling time vs. core number have been included in the operations summary for some sites.

There are, however, a number of other factors which influence the rate of penetration, so it is not always straightforward to relate rotating time directly to the hardness of the formation. First, the driller may vary the weight on the drill bit between 5,000 and 40,000 lb. Typically weight on bit is increased gradually downhole. Secondly, the rate of rotation of the bit can be varied between about 10 and 160 revolutions per minute (RPM). Finally, the rate at which seawater is circulated out the bottom of the pipe can be adjusted over a wide range. The parameters of rotating time, bit weight, speed of rotation, pump pressure, flow rate, and torque of the pipe are recorded on the rig floor and are discussed in the "Operations" section of each site chapter where they are thought to reveal geologic insight.

In the case of advanced piston cores, one other phenomenon observed by the driller is of interest: after the piston corer is seated at the base of the pipe, the driller pumps seawater into the pipe until the pressure in the pipe forces the piston corer explosively into the sediment, shearing off several metal pins which had been holding it in place. Ideally the pressure in the pipe should increase gradually and then drop off almost instantaneously during this procedure. If, however, the resistance of the mud decelerates the corer too abruptly, before it can penetrate a full core length into the sediment, the driller will observe a gradual rather than sudden decrease in pressure or, more commonly, that the pressure fails to bleed off downhole and must be relieved by opening a valve on the deck. In these cases, although the corer may come up full, part of the recovered material will be flow-in. The occurrence of flow-in was noted on the visual core description forms when inferred from drilling characteristics and/or visual observation of the split core.

SHIPBOARD SCIENTIFIC PROCEDURES

Numbering of Sites, Holes, Cores, and Samples

ODP drill sites are numbered consecutively from the first site drilled by *Glomar Challenger* in 1968. Site numbers are slightly different from hole numbers. A site number refers to one or more holes drilled while the ship is positioned over a single acoustic beacon. Several holes may be drilled at a single site by pulling the drill pipe above the seafloor (out of one hole), moving the ship some distance from the previous hole, and then drilling another hole.

For all ODP drill sites, a letter suffix distinguishes each hole drilled at the same site. For example, the first hole takes the site number with suffix A, the second hole takes the site number with suffix B, and so forth. This procedure is different from that used by the Deep Sea Drilling Project (Sites 1-624) and prevents ambiguity between site and hole number designations.

The cored interval is measured in meters below the seafloor (Fig. 1). The depth interval of an individual core is the depth below seafloor at which the coring operation began to the depth below seafloor at which the coring operation ended. Each coring interval is as long as 9.7 m, which is the maximum lineal capacity of a core barrel. The coring interval may, however, be shorter. "Cored intervals" are not necessarily adjacent to each other but may be separated by "drilled intervals." In soft sediment, the drill string can be "washed ahead" with the core barrel in place, but not recovering sediment, by pumping water down the pipe at high pressure to wash the sediment out of the way of the bit and up the space between the drill pipe and wall of the hole; however, if thin, hard rock layers are present, it is possible to get "spotty" sampling of these resistant layers within the washed interval.

Cores taken from a hole are numbered sequentially from the top of the hole downward. Maximum full recovery for a single

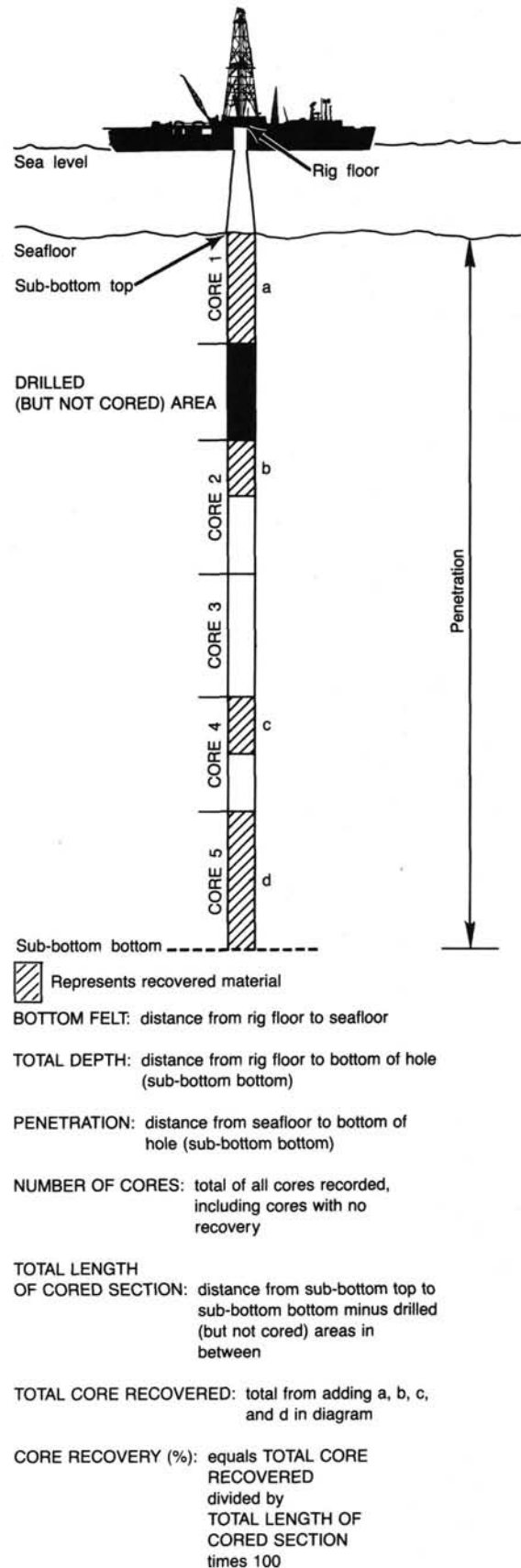


Figure 1. Diagram illustrating terms used in discussion of coring operations and core recovery.

core is 9.7 m of sediment or rock in a plastic liner (6.6 cm in diameter), plus a sample about 0.2 m long (without a plastic liner) in a core catcher. The core catcher is a device at the bottom of the core barrel which prevents the core from sliding out when the barrel is being retrieved from the hole. The sediment core, which is in the plastic liner, is then cut into 1.5-m-long sections which are numbered sequentially from the top of the sediment core (Fig. 2); the routine for handling hard rocks is described in the section on "Basement Rocks" below. With full recovery, the sections are numbered from 1 through 7, the last section being shorter than 1.5 m. For sediments and sedimentary rocks, the core catcher sample is placed below the last section and treated as a separate section. For igneous and metamorphic rocks, material recovered in the core catcher is included at the bottom of the last section.

When recovery is less than 100%, whether or not the recovered material is contiguous, the recovered sediment is placed at the top of the cored interval, and then 1.5-m-long sections are numbered sequentially, starting with Section 1 at the top. There will be as many sections as needed to accommodate the length of the core recovered (Fig. 2); for example, 3 m of core sample in a plastic liner will be divided into two 1.5-m-long sections. Sections are cut starting at the top of the recovered sediment, and the last section may be shorter than the normal 1.5-m length. If, after the core has been split, fragments which are separated by a void appear to have been contiguous *in situ*, a note is made in the description of the section. All voids, whether real or artificial, are curatorially preserved and noted in the barrel sheets.

Samples are designated by distances in centimeters from the top of each section to the top and bottom of the sample interval in that section. A full identification number for a sample consists of the following information: (1) leg, (2) site, (3) hole, (4) core number and type (see below), (5) section, and (6) interval in centimeters. For example, the sample identification number "107-

652A-3R-2, 98-100 cm" means that a sample was taken between 98 and 100 cm from the top of Section 2 of rotary-drilled Core 3, from the first hole drilled at Site 652 during Leg 107. A sample from the core catcher (CC) of this core might be designated "107-652A-3R, CC, 8-9 cm."

The depth below the seafloor for a sample numbered, for example, "107-652A-3R-2, 98-100 cm" is the sum of the depth to the top of the cored interval for Core 3 (11.8 m) plus the 1.5 m included in Section 1 plus the 98 cm below the top of Section 2. The sample in question is therefore located at 14.28 m sub-bottom which, in principle, is the sample sub-seafloor depth (sample requests should refer to a specific interval within a core section, rather than sub-bottom depths in meters).

In Core 651A-1R, we cored 3.7 m but recovered 9.5 m (see "Site 651" chapter, this volume). That this recovery is greater than the interval cored is attributed to soft sediment expanding up into the barrel because the diameter of the hole drilled was greater than the diameter of the core liner. To assign sub-bottom depths to Core 651A-1R, we apportion the 9.5 m recovered equally to the 3.7-m drilled interval (0-3.7 mbsf).

All ODP core and sample identifiers include "core type." The following abbreviations are used: R = rotary barrel; H = advanced piston core (APC), P = pressure core barrel; X = extended core barrel (XCB); B = drill-bit recovery; C = center-bit recovery; I = *in-situ* water sample; S = sidewall sample; W = wash core recovery; and M = miscellaneous material. APC, XCB, and RCB cores were drilled on Leg 107.

Core Handling

As soon as a core was retrieved on deck, a sample was taken from the core catcher and taken to the paleontological laboratory for an initial assessment of the age of the sample.

The core was then placed on the long horizontal rack and gas samples were taken by piercing the core liner and withdrawing gas into a vacuum-tube sampler. Voids within the core were sought as sites for the gas sampling. The gas samples were analyzed immediately, as part of the shipboard safety and pollution-prevention program. Next, the core was marked into section lengths, each section was labeled, and the core was cut into sections. Interstitial water (IW) and organic geochemistry (OG) whole-round samples were then taken. Each section was sealed top and bottom by gluing on a plastic cap, blue to identify the top of a section and clear for the bottom. A yellow cap was placed on both section ends from which a whole-round core sample had been removed. The caps were usually attached to the liner by coating the end of the liner and the inside rim of the end cap with acetone, though we elected to tape the end caps in place without acetone at geochemically-interesting portions.

The cores were then carried into the laboratory, where the sections were again labeled using an engraver to mark the full designation of the section. The length of core in each section and the core-catcher sample was measured to the nearest centimeter, and this information was logged into the shipboard core-log database program.

The cores were then allowed to warm to room temperature (approximately 4 hr) before they were split. During this time, the whole-round sections were run through the gamma ray attenuation porosity evaluation (GRAPE) device for estimating bulk density and porosity (see below; Boyce, 1976) and, in some cases, through the three-axis, pass-through cryogenic rock magnetometer (see below). After the cores had equilibrated to room temperature, thermal conductivity measurements were made using the needle probe method before splitting.

Cores of relatively soft material were split lengthwise into *work* and *archive* halves. The softer cores were split with a wire or (depending on the degree of induration) a saw, using shipboard water. In soft sediments, some smearing of material can occur

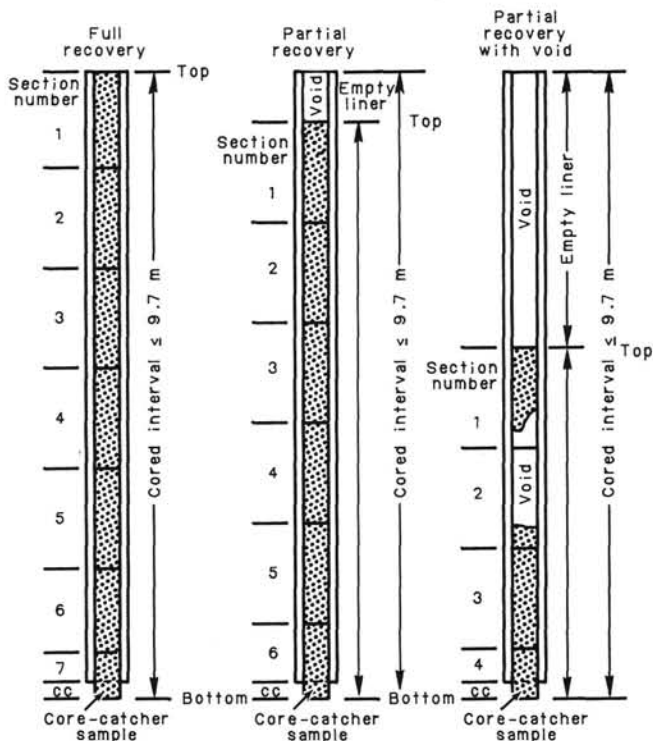


Figure 2. Diagram showing procedure for cutting and numbering recovered core sections.

and, to minimize contamination, scientists analyzing samples should avoid using the very near-surface part of the split core. Harder cores were split with a band saw or diamond saw. Where the cored material was of uneven diameter, or did not fill the entire diameter of the core liner, the diameter of the split core was measured with calipers at all significant points to provide the path-length data needed later to interpret the GRAPE data. These caliper data were recorded on the visual core description forms.

The *work* half was sampled for both shipboard and shore-based laboratory studies. Each extracted sample was listed by location and the name of the investigator receiving the sample and logged into the sampling computer program. Records of all removed samples are kept by the Curator at ODP. The extracted samples were sealed in plastic vials or bags and labeled. Samples were routinely taken for shipboard analysis of sonic velocity by the Hamilton Frame method, water content by gravimetric analysis, percent calcium carbonate (CO₂ coulometer), and other purposes. Many of these data are reported in the site chapters.

The *archive* half was described visually. Smear slides were made from samples taken from the *archive* half, and were supplemented by thin sections taken from the *work* half. The *archive* half was then photographed with both black and white and color film, a whole core at a time.

Both halves were then put into labeled plastic tubes, sealed, and transferred to cold-storage space aboard the drilling vessel. Leg 107 cores were taken from the ship via refrigerated transport to cold storage at the East Coast Repository, at Lamont-Doherty Geological Observatory, Palisades, NY.

SEDIMENT CORE DESCRIPTION FORMS (“BARREL SHEETS”)

The core description forms (Fig. 3), or “barrel sheets,” summarize the data obtained during shipboard analysis of each core. The following discussion explains the ODP conventions used in compiling each part of the core description form, and the exceptions to these procedures adopted by Leg 107 scientists.

Core Designation

Cores are designated using site, hole, and core number and type as previously discussed (see “Numbering of Sites, Holes, Cores, and Samples” above). In addition, the cored interval is specified in terms of meters below sea level (mbsl) and meters below sea floor (mbsf). On Leg 107, these depths were based on the drill pipe measurement, as reported by the SEDCO/FOREX Coring Technician and the ODP Operations Superintendent.

Age Data

Microfossil abundance, preservation, and zone assignment, as determined by the shipboard paleontologists, appear on the core description form under the heading “Biostrat. Zone/Fossil Character.” The geologic age determined from the paleontological and/or paleomagnetic results appears in the “Time-Rock Unit” column.

On Leg 107 calcareous nannofossils and planktonic and benthic foraminifers provided the majority of age determinations. Detailed information on the zonations and terms used to report abundance and preservation appear below (see “Biostratigraphy” section, this chapter).

Paleomagnetic, Physical Property, and Chemical Data

Columns are provided on the core description form to record paleomagnetic results, location of physical properties samples (density, porosity, and velocity), and chemical data (percentage of CaCO₃ determined using the CO₂ coulometer). Additional information on shipboard procedures for collecting these types

of data appears below (see “Paleomagnetism,” “Physical Properties,” and “Geochemistry” sections, this chapter).

Graphic Lithology Column

The lithological classification scheme presented here is represented graphically on the core description forms using the symbols illustrated in Figure 4. We have made the following modifications and additions to the graphic lithology representation scheme that was recommended by the JOIDES Sedimentary Petrology and Physical Properties Panel.

A thick, horizontal line identifies thin (<10 cm) sapropel (s), foraminifer sands, and volcanic ash (v) layers. Where double letters are used, two or more layers are present. Note that the thickness of the horizontal line does not imply a layer thickness, rather this line simply identifies the stratigraphic position of the layer(s). Pumice fragments of lapilli or block-sizes are identified by a circle containing a “v.” A simple symbol may represent numerous fragments, and in some cases (e.g., 650) an entire core section filled with pumice. Where ash and sapropel are interbedded, a “s/v” designation is made. A circle surrounding a “c” defines sediments containing 15%–30% CaCO₃ (transitional calcareous biogenic sediments, see “Sediment Classification” section below). Biogenic sands (such as foraminifer sands) are indicated by the CB10 symbol wherever these deposits are 10 cm thick or more. Sapropel layers (> 10 cm thick) are represented by solid black intervals.

Note that sediment types portrayed on the graphic lithology column are based upon smear slide criteria. These criteria tend to underestimate foraminifers, as a result of larger test sizes which are often difficult to incorporate on smear slides of typically finer grained, deep-sea sediments, thus biogenic ooze designations underrepresent the foraminifer component.

It is important to realize that the ODP conventions for graphically representing sediment types do not distinguish a sequence of mixed components (e.g., 50% calcareous ooze, 50% clay) from a sequence of thin (<10 cm) interbedded sediments of each component (e.g., alternating calcareous ooze and clay layers).

Sediment Disturbance

Core deformation probably occurs during one of three different steps at which the core can suffer stresses sufficient to alter its physical characteristics: cutting, retrieval (with accompanying changes in pressure and temperature), and core handling.

The coring technique, which uses a 25-cm-diameter bit with a 6-cm-diameter core opening, may result in extreme disturbance of the recovered core material. This is illustrated in the “Drilling Disturbance” column on the core description form using the symbols in Figure 5, as explained below.

The following disturbance categories are recognized for soft and firm sediments:

1. Slightly deformed: bedding contacts are slightly bent.
2. Moderately deformed: bedding contacts have undergone extreme bowing.
3. Highly deformed: bedding is completely disturbed, sometimes showing symmetrical diapirlike structure, biscuits may occur.
4. Soupy: intervals are water saturated and have lost all aspects of original bedding.

The following categories are used to describe the degree of fracturing in hard sediments and igneous and metamorphic rocks (Fig. 5):

1. Slightly fractured: core pieces in place, with very little drilling slurry or breccia.

SITE		HOLE				CORE		CORED INTERVAL					
TIME-ROCK UNIT	BIOSTRAT. ZONE / FOSSIL CHARACTER				PALEOMAGNETICS	PHYSICAL PROPERTIES	CHEMISTRY	SECTION	METERS	GRAPHIC LITHOLOGY	DRILLING DISTURB. SED. STRUCTURES	SAMPLES	LITHOLOGIC DESCRIPTION
	FORAMINIFERS	NANNOFOSSILS	RADIOLARIANS	DIATOMS									
								0.5					
							1	1.0					
							2						
							3						
							4						
							5						
							6						
							7						
							CC						

PRESERVATION:
 G = Good
 M = Moderate
 P = Poor

ABUNDANCE:
 A = Abundant
 C = Common
 F = Frequent
 R = Rare
 B = Barren

Velocity, porosity, and density
 Carbonate (%)

See key to graphic lithology symbols (Figure 4)

See key to symbols in Figures 5 and 6

OG ← Organic geochemistry sample

Smear-slide summary (%):
 Section, depth (cm)
 M = minor lithology, D = dominant lithology

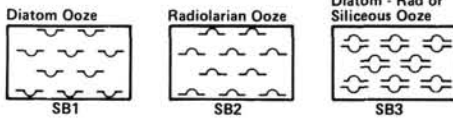
IW ← Interstitial water sample

* ← Smear slide

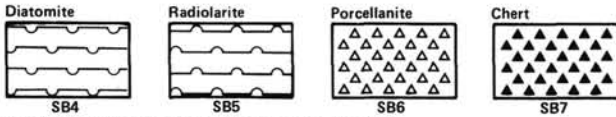
Figure 3. Core description form ("barrel sheet") used for sediments and sedimentary rocks.

PELAGIC SEDIMENTS

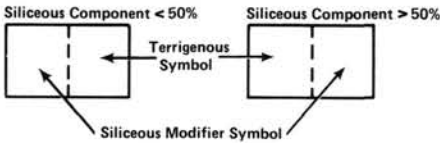
Siliceous Biogenic Sediments
PELAGIC SILICEOUS BIOGENIC - SOFT



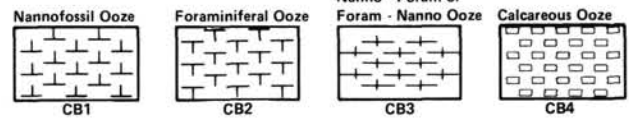
PELAGIC SILICEOUS BIOGENIC - HARD



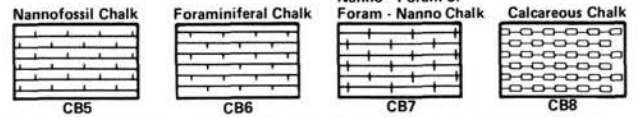
TRANSITIONAL BIOGENIC SILICEOUS SEDIMENTS



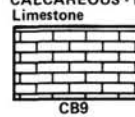
Calcareous Biogenic Sediments
PELAGIC BIOGENIC CALCAREOUS - SOFT



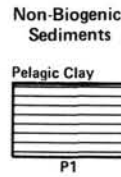
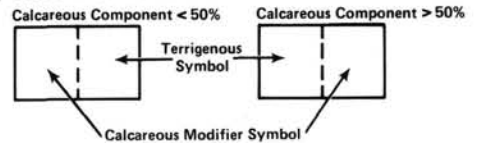
PELAGIC BIOGENIC CALCAREOUS - FIRM



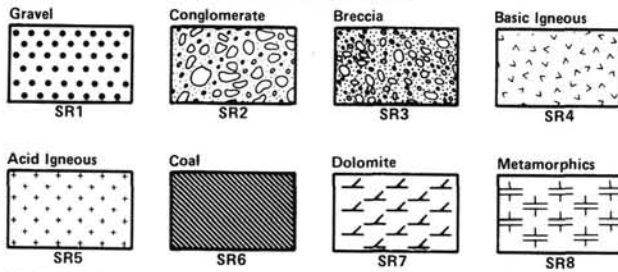
PELAGIC BIOGENIC CALCAREOUS - HARD



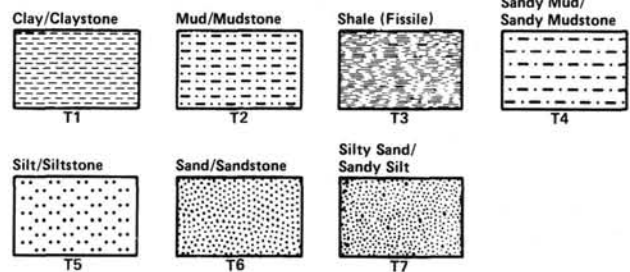
TRANSITIONAL BIOGENIC CALCAREOUS SEDIMENTS



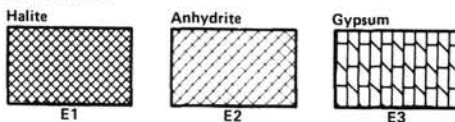
SPECIAL ROCK TYPES



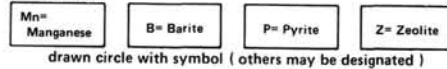
TERRIGENOUS SEDIMENTS



EVAPORITES



Concretions



VOLCANOGENIC SEDIMENTS

LAYERS

- S = Sapropel
- V = Volcanic ash
- (V) = Pumice fragments
- (C) = 15%-30% C₂CO₃

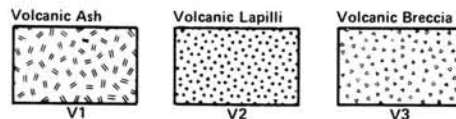


Figure 4. Key to lithologic symbols used in "Graphic Lithology" column on core description forms (see Fig. 3).

2. Moderately fragmented: core pieces in place or partly displaced, but original orientation is preserved or recognizable. Drilling slurry may surround fragments.

3. Highly fragmented: pieces are from the interval cored and probably in correct stratigraphic sequence (although they may not represent the entire section), but original orientation is totally lost.

4. Drilling breccia: core pieces have completely lost their original orientation and stratigraphic position. May be completely mixed with drilling slurry.

Sedimentary Structures

In soft and even in some harder sedimentary cores, it may be extremely difficult to distinguish between natural structures and structures created by the coring process. However, where such structures were observed, they are indicated on the "Sedimentary Structure" column of the core description forms. A key to the structural symbols used on Leg 107 is given in Figure 6. We have added two new symbols: an "L" indicates a lithified sediment or nodule, and a series of parallel wavy lines identifies a

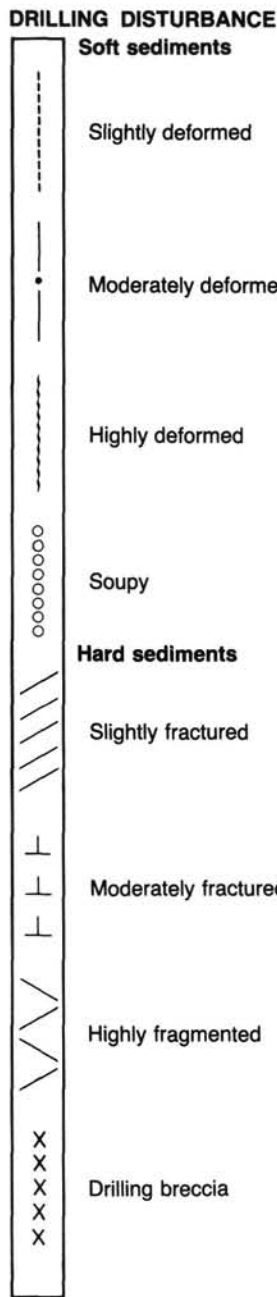


Figure 5. Drilling disturbance symbols used on Leg 107 core description forms.

sequence of thin (on the order of millimeters) parallel or near-parallel lamination.

Samples

The position of samples taken from each core for shipboard analysis is indicated in the "Samples" column in the core description form. An asterisk (*) indicates the location of smear slide samples. The symbols IW and OG designate whole-round interstitial water, and frozen organic geochemistry samples, respectively.

The position of samples for routine physical properties analyses are indicated by a dot in the "Physical Properties" column; the location of samples for CO₂ coulometer analyses are indicated by a dot in the "Chemistry" column (these samples are

SEDIMENTARY STRUCTURES

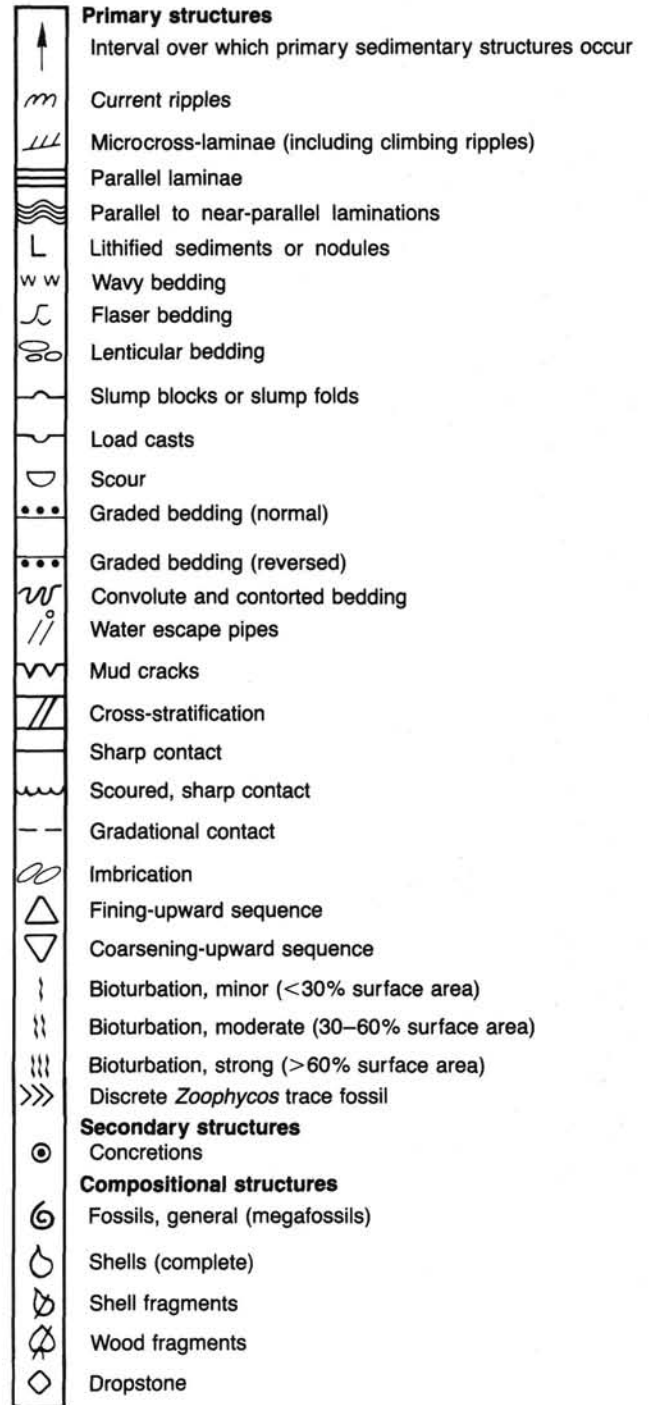


Figure 6. Sedimentary structure symbols for sediments and sedimentary rocks.

taken from the working half of the core, and generally correspond to smear slide locations in the archive half, although this is not always the case). Carbonate content and physical properties data are given beside the sample dots.

Lithologic Description—Text

The lithologic description which appears on each core description form consists of two parts: (1) a brief heading which

lists the lithologies (as determined using the sediment classification scheme discussed below) observed in a given core in order of importance or dominance, and (2) a detailed description of these lithologies.

Smear Slide Summary

A table summarizing smear slide and thin section data appears on each core description form. The section and interval from which the sample was taken is noted, as well as identification as a dominant (D) or minor (M) lithology in the core. The percent of all identified components (totalling 100%) is listed. As explained below, these data, combined with CaCO₃ measurements done on board, are used to classify the recovered material. It is important to note that smear slide estimates are not corrected to CaCO₃ content, thus the smear slide data are in error in some cases.

OBTAINING SAMPLES

Potential investigators wishing to obtain samples should refer to the ODP-NSF Sample Distribution Policy. Sample request forms may be obtained from the Curator, Ocean Drilling Program, Texas A&M University, College Station, Texas 77843-3469. Requests must be as specific as possible: include site, hole, core, section, interval within a section, and volume of sample required.

SEDIMENT CLASSIFICATION

The classification system used during Leg 107 was a modification of that devised by the Joint Oceanographic Institutions for Deep Earth Sampling (JOIDES) former Panel on Sedimentary Petrology and Physical Properties (SP⁴) and adopted for use by the JOIDES Planning Committee in March 1974. Core descriptions, smear slide descriptions, and CO₂ coulometer (percentage of CaCO₃) data, all obtained on the ship, served as the bases of the graphic core descriptions presented on the core description forms at the end of each site chapter.

Sediment and rock names were defined solely on the basis of composition and texture. Composition is most important for description of those deposits more characteristic of open marine conditions, with texture becoming more important for the classification of hemipelagic and nearshore facies. These data were primarily determined on the ship by: (1) visual estimates in smear slides and thin sections using microscopes; (2) visual observation using a hand lens, and (3) unaided visual observation. Calcium carbonate content was estimated in smear slides and by using the CO₂ coulometer technique. Other geologic features determined were color, sedimentary structures, and degree of lithification.

Color

Colors of the recovered material were determined with Munsell soil color charts. Colors were determined immediately after the cores were split and while they were still wet. Information on core colors is given in the "Lithologic Description" text on the core description forms (Fig. 3).

Firmness

The determination of induration is highly subjective, but the categories used on Leg 107 are thought to be practical and significant. The criteria of Gealy et al. (1971) were used for calcareous deposits with more than 50% CaCO₃; subjective estimate of behavior in core cutting was used for transitional calcareous sediments with less than 50% CaCO₃, pelagic, hemipelagic, and terrigenous sediments. There are three classes of firmness for calcareous sediments:

1. *Soft*: sediments which have little strength and are readily deformed under the finger or broad blade of the spatula are termed *ooze*.

2. *Firm*: partly lithified ooze or friable limestone is called *chalk*. Chalks are readily deformed under the fingernail or the edge of a spatula blade.

3. *Hard*: Indurated chalk; *Limestone* is restricted to nonfriable cemented rock.

There are only two classes of firmness for noncalcareous sediments:

1. *Soft*: sediment core may be split with a wire cutter. Soft terrigenous sediment, pelagic clay, and transitional calcareous biogenic sediments are termed *sand*, *silt*, *clay*, or *mud*.

2. *Hard*: the core is hard (i.e., consolidated or well indurated) if it must be cut with a band saw or diamond saw. For these materials, the suffix *-stone* is added to the soft-sediment name (e.g., *sandstone*, *siltstone*, *claystone*, *mudstone*).

Basic Sediment Types

Adapted and modified from the standard DSDP sediment classification scheme (Supko et al., 1978), the following defines compositional class boundaries and the use of qualifiers in the lithologic classification scheme used during Leg 107 (Fig. 7).

Pelagic Clay

Pelagic clay is fine-grained sediment that has settled through the water column, normally at very slow rates. This type of sediment has often been termed "brown clay" or "red clay." Since there is no carbonate compensation depth in the Tyrrhenian Sea, this category was not applicable during Leg 107.

Siliceous Biogenic Sediments

Siliceous biogenic sediments are distinguished from pelagic clay because they contain siliceous microfossils. Siliceous biogenic sediments are distinguished from calcareous biogenic sediments by a calcium carbonate content of less than 30%.

Since the two previous sediment types were not recovered during Leg 107, details of their classification are not given here, but can be found in most of the DSDP Initial Report explanatory notes, or in Ocean Drilling Program (1985).

Calcareous Biogenic Sediments

Calcareous biogenic sediment is distinguished by a biogenic CaCO₃ content in excess of 30%. There are two classes: (1) *pelagic calcareous biogenic sediments* which contain 65%–100% biogenic CaCO₃ (less than 30% silt and clay), and (2) *transitional calcareous biogenic sediments* which contain 30%–60% CaCO₃ (greater than 30% silt and clay). Lithologic names given to these classes of sediment are also dependent on the degree of sediment consolidation, as shown in Figure 4. Sediments belonging to other classification categories, but which contain 10%–30% of calcareous components, are given the modifier "calcareous" (or "foraminiferal" or "nannofossil," as appropriate). In the graphic lithology description on the barrel sheets, these sediments are identified by a "C" within a circle. Less than 10% CaCO₃ was ignored in the sediment nomenclature.

1. Pelagic Biogenic Calcareous Sediments: (a) *Soft*: calcareous oozes; (b) *Firm*: chalk; and (c) *Hard*: indurated chalk. The term "Limestone" is restricted to cemented rocks.

Composition qualifiers: Principal components are nannofossils and foraminifers. One or two qualifiers were commonly used, for example:

Foraminifers (%)	Name
< 10:	Nannofossil ooze, chalk, limestone
10–25:	Foraminiferal-nannofossil ooze
25–50:	Nannofossil-foraminiferal ooze
> 50:	Foraminiferal ooze

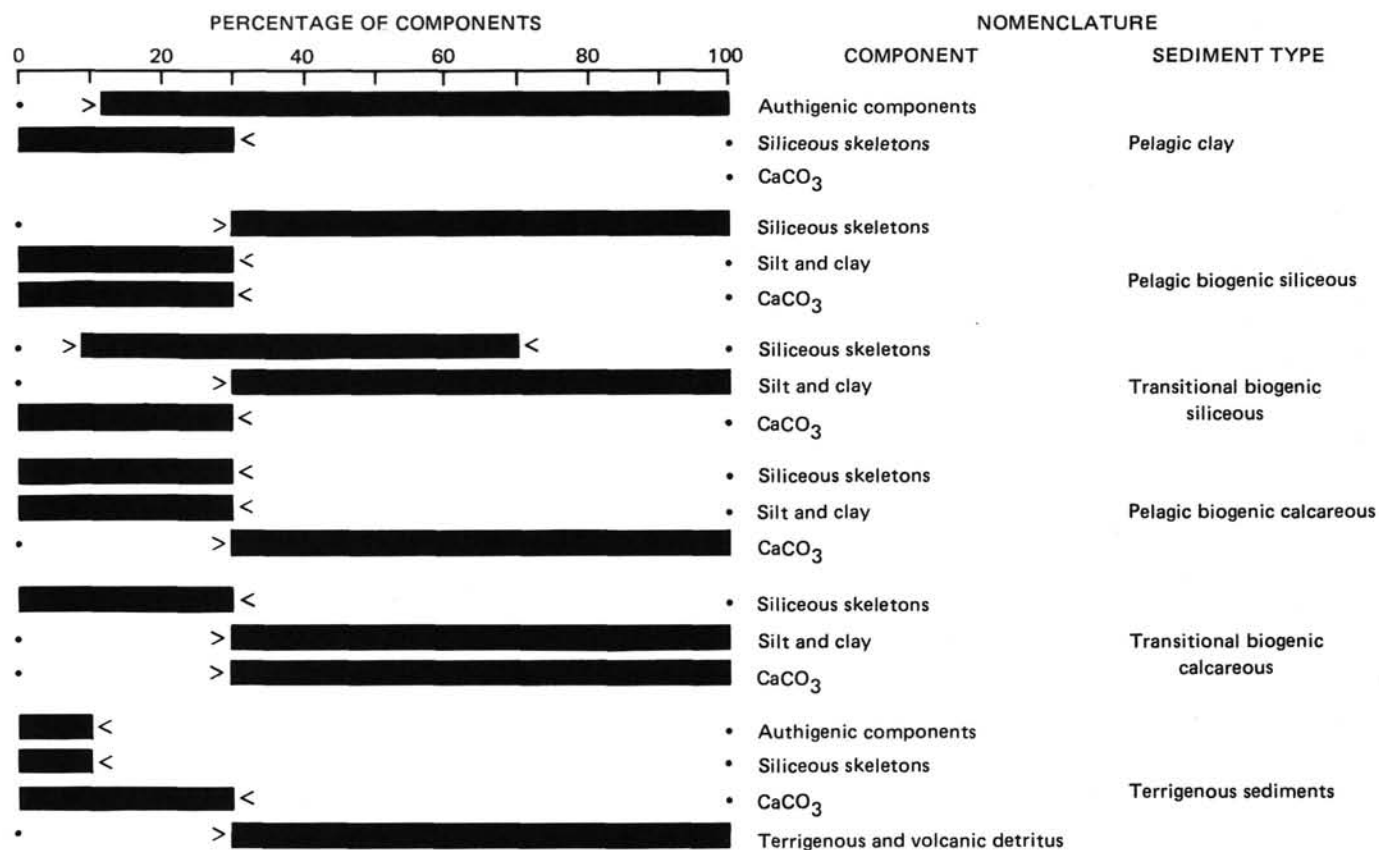


Figure 7. Summary chart for lithologic classification of sediments.

2. Transitional Biogenic Calcareous Sediments: (a) Soft: marly calcareous (or nannofossil, foraminifer, etc.) ooze; (b) Firm: marly chalk; and (c) Hard: marly limestone.

Terrigenous Sediments:

Sediments falling in this portion of the classification scheme are divided into textural groups on the basis of the relative proportions of three grain-size constituents, i.e., sand, silt, and clay. Coarser terrigenous sediments were classed as conglomerate or breccia, clast-supported or matrix-supported, and are treated as "Special Rock Types" (Fig. 4). The size limits for these constituents are those defined by Wentworth (1922) (Fig. 8).

Five major textural groups are recognized on the accompanying triangular diagram (Fig. 9). The groups are defined according to the abundance of clay (>90%, 90%-10%, <10%) and the ratio of sand to silt (>1 or <1). Terms such as *clay*, *silty clay*, *sandy clay*, *clayey silt*, *clayey sand*, *silt*, and *sand* are used for unconsolidated sediments which could be cut with a wire in the shipboard core-splitting process. The hard or consolidated equivalents for the same textural groups are *claystone*, *silty claystone*, *sandy claystone*, *clayey siltstone*, *clayey sandstone*, *siltstone*, and *sandstone*. Sedimentary rocks are those which had to be cut with the band saw or diamond saw.

In this sediment category, numerous qualifiers are possible, usually based on minor constituents (for example, "glauconitic," "pyritic," "feldspathic"). Terrigenous sediments and sedimentary rocks containing 10%-30% CaCO₃ are qualified by the modifier "calcareous."

Volcanogenic Sediments:

Pyroclastic rocks are described according to the textural and compositional scheme of Schmid (1981). The textural groups

are: (1) volcanic block breccia (greater than 64 mm in size); (2) volcanic lapilli (2-64 mm in size); and, (3) volcanic ash, tuff if indurated (less than 2 mm in size). Compositionally, these pyroclastic rocks are described as vitric (glass), crystal, or lithic.

Clastic sediments of volcanic provenance are described in the same fashion as terrigenous sediments, noting the dominant composition of the volcanic grains where possible.

Special Sediment Rock Types

Several special sedimentary and metasedimentary rock types (not included in the classification scheme described above) were recovered during Leg 107:

Halite, anhydrite, gypsum (as a rock)
Sapropels
Gravel, conglomerate, breccias
Pumice, quartzite, marble, greenschist, metaquartzite.

IGNEOUS AND METAMORPHIC ROCK CLASSIFICATION

Igneous rocks were classified mainly on the basis of hand-specimen mineralogy and texture. Thin-section study provided additional information to the hand-specimen classification, and allowed for detailed assessment of such features as the type and extent of alteration. Basalts, dolerites, metadolerites, serpentinized peridotites, and granodiorites were the main igneous rock types recovered on Leg 107.

Basement Rock Handling

Igneous and metamorphic rocks were split, using a rock saw with a diamond blade, into *archive* and *work* halves. The *work*

MILLIMETERS	μm	PHI (Φ)	WENTWORTH SIZE CLASS
4096		-20	
1024		-12	Boulder (-8 to -12 Φ)
256		-8	
64		-6	Cobble (-6 to -8 Φ)
16		-4	Pebble (-2 to -6 Φ)
4		-2	
3.36		-1.75	
2.83		-1.5	Granule
2.38		-1.25	
2.00		-1.0	
1.68		-0.75	
1.41		-0.5	Very coarse sand
1.19		-0.25	
1.00		0.0	
0.84		0.25	
0.71		0.5	Coarse sand
0.59		0.75	
1/2	500	1.0	
0.42	420	1.25	
0.35	350	1.5	Medium sand
0.30	300	1.75	
1/4	250	2.0	
0.210	210	2.25	
0.177	177	2.5	Fine sand
0.149	149	2.75	
1/8	125	3.0	
0.105	105	3.25	
0.088	88	3.5	Very fine sand
0.074	74	3.75	
1/16	63	4.0	
0.053	53	4.25	
0.044	44	4.5	Coarse silt
0.037	37	4.75	
1/32	31	5.0	
1/64	15.6	6.0	Medium silt
1/128	7.8	7.0	Fine silt
1/256	3.9	8.0	Very fine silt
0.0020	2.0	9.0	
0.00098	0.98	10.0	Clay
0.00049	0.49	11.0	
0.00024	0.24	12.0	
0.00012	0.12	13.0	
0.00006	0.06	14.0	

Figure 8. Grain size categories used for classification of terrigenous sediments (from Wentworth, 1922).

halves were described and sampled on board ship. Each piece of rock was numbered sequentially from the top of each core section, beginning with the number 1. Pieces were labeled on the rounded, not the sawed, surface. Pieces that could be fitted together before splitting were given the same number, but were lettered consecutively downsection, as 1A, 1B, 1C, and so on. Spacers were placed between pieces with different numbers, but not between those with different letters and the same number. In general, spacers represent drilling gaps (no recovery). All pieces which were cylindrical when recovered and of greater length than the diameter of the liner have orientation arrows pointing to the top of the section, both on *archive* and *work* halves. Special procedures were used to ensure that orientation was preserved through every step of the sawing and labeling process.

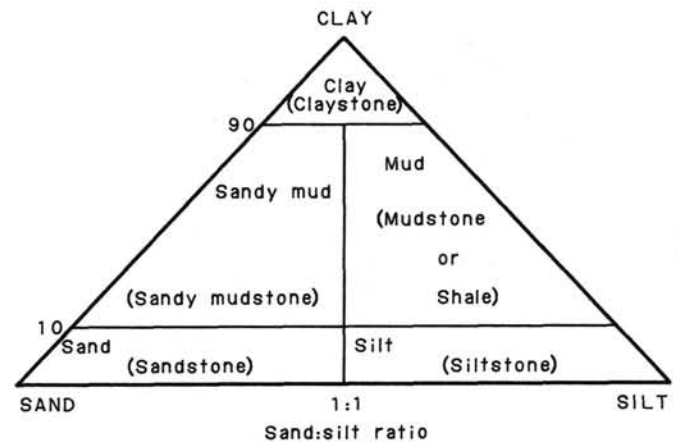


Figure 9. Triangular diagram showing classification scheme used for terrigenous sediments and sedimentary rocks on Leg 107.

Core Description Form

The core description forms used for igneous and metamorphic rocks are not the same as those used for sediments and sedimentary rocks. Igneous rock representation on standard sediment core description forms (i.e., Fig. 3) would be too compressed to provide adequate information for potential sampling. Consequently, special core description forms are used for more complete graphic representation (Fig. 10). Graphic representatives of each 1.5-m section of core are shown on these forms, as well as summary hand-specimen and thin-section descriptions. The symbols and a number of format conventions for igneous rocks are presented on Figure 10.

Microstructural Pattern

The top of the form contains the section identification information. Piece numbers, core diameters, and a graphic representation of the section are noted on the left side of the form. The graphic representation includes outlines and obvious features of the pieces (oxidation haloes, foliations, fractures, lineations, textures). All pieces suitable for sampling programs that require known orientations are indicated by upward-pointing arrows on the igneous and metamorphic core description forms. Samples taken for shipboard studies are noted by their sample abbreviation at the corresponding interval: T for thin section, XRF for X-ray fluorescence, XRD for X-ray diffraction. The degree of alteration is indicated with the symbols shown in Figure 11.

S_1, S_2, S_3, \dots identify the successive foliations with their orientation and dip.

L_1, L_2, L_3, \dots are used to characterize the lineations by their orientation on the foliation plane.

F_1, F_2, F_3, \dots characterize the successive fracture planes. The orientation, the dip of the plane, the sense of motion (N, tensional; I, reverse; S, sinistral; D, dextral), and when possible the pitch of slickensides are indicated.

In general, the orientation of cores is unknown. Orientations of microstructures were measured in reference to the section plane, which will be used as a further reference (i.e., for paleomagnetic measurements).

Basalt Nomenclature

Shipboard classification of basalts is based mainly on mineralogy and texture. Basalts are termed aphyric, sparsely phytic, moderately phytic, or highly phytic, depending on the proportion of phenocrysts.

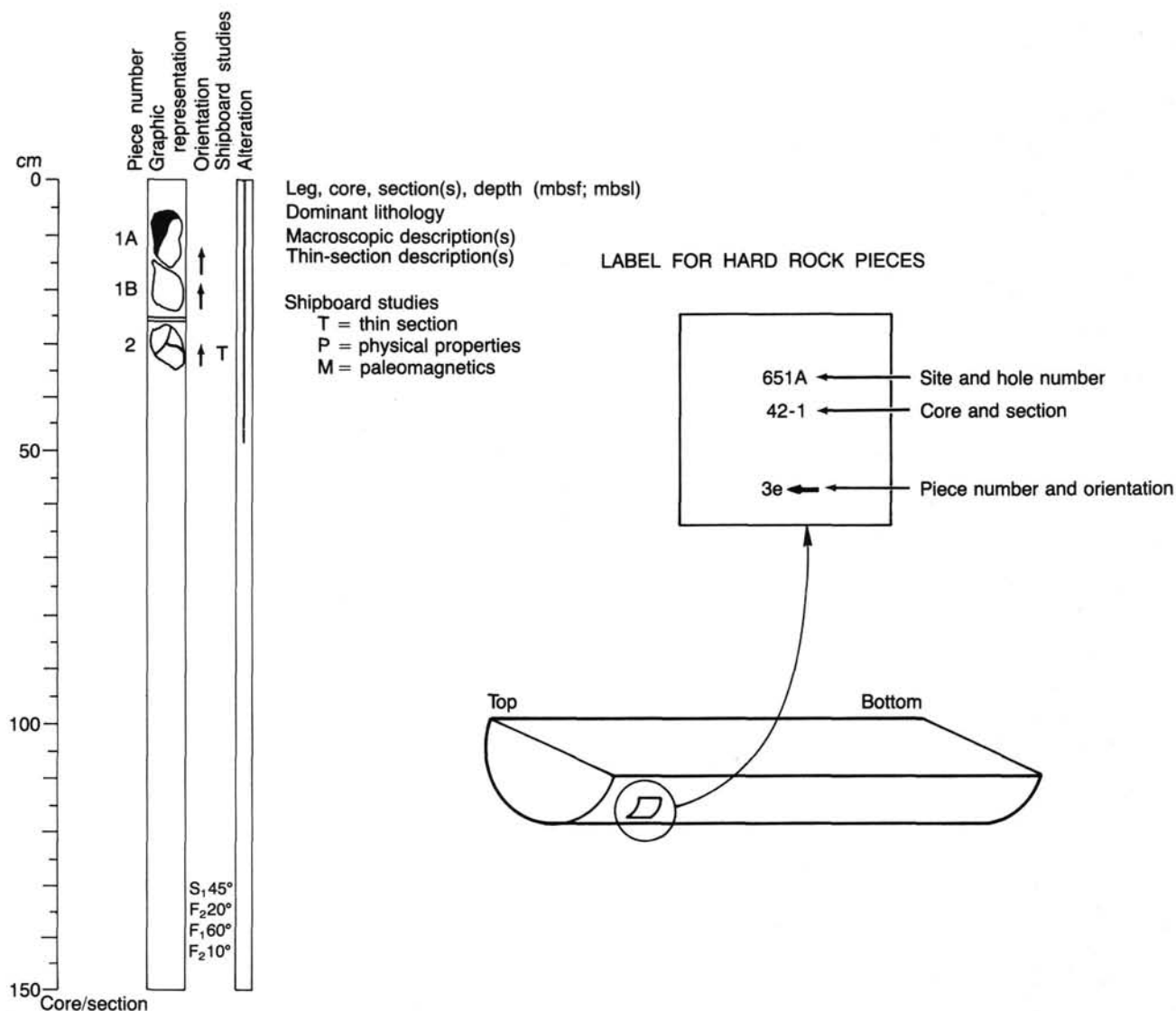


Figure 10. Core description forms used for igneous and metamorphic rocks.

Aphyric basalts contain no phenocrysts. For practical purposes, if one piece of basalt is found with a phenocryst or two in a section where all other pieces lack phenocrysts, and no other criteria such as grain size or texture distinguish this basalt from the others, then it is described as aphyric. A note of the rare phenocrysts is included in the general description. This approach enables us to restrict the number of lithologic units to those with clearly distinctive and persistent visible differences.

Sparsely phyrlic basalts are those with 1%–2% phenocrysts in almost every piece of a given core or section. Clearly contiguous pieces without phenocrysts are included in this category and the lack of phenocrysts is noted in the general description. Moderately phyrlic basalts contain 2%–10% phenocrysts. Phyrlic basalts contain more than 10% phenocrysts. No separate designation is made for basalts with more than 20% phenocrysts; the proportion indicated in the core forms should be sufficient to guide the reader.

The basalts are further classified by phenocryst type, and a modifying term follows the terms phyrlic, sparsely phyrlic, etc.

For example, a moderately phyrlic plagioclase-olivine basalt contains 2%–10% phenocrysts, most of them olivine, but with some plagioclase, i.e., the least abundant phenocryst phase is listed first.

Lithologic Units—Basalts

1. Massive units: the core is commonly affected little by drilling and is recovered in long intact pieces.
2. Dikes: units with one or two chilled intrusive margins.
3. Sheet flows: units characterized by parallel, closely-spaced (under 0.5 m apart), mainly horizontal, flat glassy selvages, distinct from the rounded or inclined margins of pillow units.
4. Thin flows: units recognized by homogeneous areas of core in excess of 1 m thick (i.e., thicker than the average pillow), formed by fine-grained basalts.
5. Pillow basalts: all core remaining after the preceding lithologic types have been identified. These are characterized by chilled pillow margins (mostly curved or inclined), hyaloclastic breccias, and fine-grained, often highly fractured rocks.

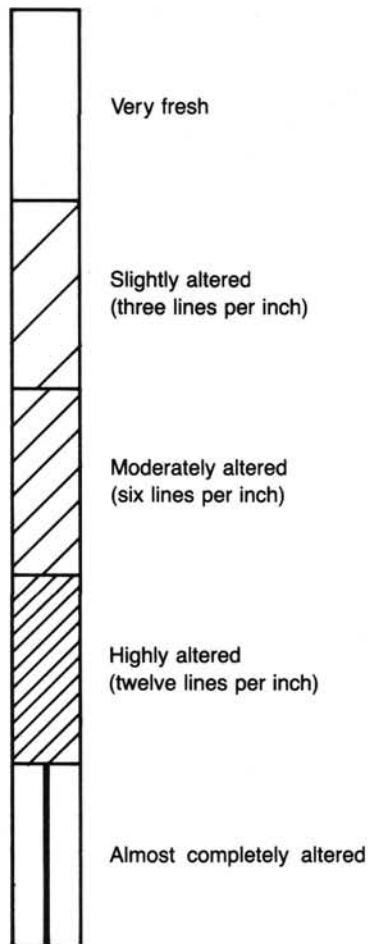


Figure 11. Alteration degree symbols used on Leg 107 in igneous and metamorphic section description forms.

Terminology and Definitions

The definitions and terminology given for igneous and metamorphic units are taken from Jackson (1970), American Geological Institute (1980), and Tomkiewf (1983).

1. Igneous Terms

A. Grain Size

Aphanitic:

A uniform texture in which individual crystals are invisible to the unaided eye.

Microcrystalline:

The texture of a rock having crystals that are small enough to be visible under a microscope.

Cryptocrystalline:

The texture of a rock having crystals too small to be resolved optically, although an aggregate birefringence may be evident.

Glassy or Hyaline:

The material is glass, in practice seldom completely free of crystallites and/or microlites.

Phaneritic:

A texture in which individual crystals are readily visible to the unaided eye.

Coarse-grained:

Crystals are larger than 5 mm in diameter.

Medium-grained:

Crystals range from 1 to 5 mm in diameter.

Fine-grained:

Crystals are visible but less than 1 mm in diameter.

B. Degree of Crystallinity

Holohyaline:

Rocks which are completely glassy and lack megascopic crystals.

Hypohyaline/hypocrystalline:

Rocks composed of crystals and glass; hypohyaline is dominantly glass, hypocrystalline is dominantly crystal.

Holocrystalline:

Rocks composed entirely of crystals.

C. Shape of Individual Crystals

Euhedral:

A crystal completely bounded by its own faces.

Subhedral:

A crystal bounded in part by its own faces and in part by surfaces developed through mutual interference of adjacent crystals.

Anhedral:

A crystal not bounded by its own crystal faces but whose form is impressed on it by adjacent crystals.

D. Rock Textures Defined By Single-Crystal Shapes

Panidiomorphic-granular:

The texture of a rock composed essentially of euhedral crystals.

Hypidiomorphic-granular:

The texture of a rock composed of a mixture of anhedral and either subhedral or euhedral crystals or both.

Allotriomorphic-granular:

The texture of a rock composed entirely of anhedral crystals. *Aplitic* texture usually implies fine grain size and sugary texture.

E. Incipient Crystals

Crystallites:

The most rudimentary form of crystals, as yet too small to have distinct mineral properties. They are seen microscopically as granules, rods, hairs, and dendritic or feathery objects. *Globulites* are spherical crystallites commonly found in volcanic glass.

Microlites:

Incipient crystals large enough to have identifiable mineral properties, although still of microscopic size. The aphanitic groundmass of extrusives is usually composed of crystals of microlite size.

Skeletal crystals:

Incompletely formed crystals in which the faces of maximum growth rate have developed leaving hollow or hopper-shaped interiors.

F. Postsolidification Features of Glasses

Perlitic structure: Concentric shelly cracks that develop in some glasses.

Devitrification: The slow process of reorganization of a glass into crystals, usually of very small size.

Spherulitic structure: Spherical bodies from microscopic size to many feet in diameter which consist of radiating fibers and plates.

Variolitic: A texture found in basic rocks in which the spherulites consist of minute, radiating fibers of plagioclase with interstitial glass, augite, olivine, or magnetite. Rocks with a variolitic structure frequently have a pitted or spotted appearance.

G. Porphyritic Textures

Glomeroporphyritic: Clumps of phenocrysts.

Intersertal: Said of the texture of a porphyritic igneous rock in which the groundmass, composed of a glassy or partly crystalline material other than augite, occupies the interstices between unoriented feldspar laths.

Microclitic: A texture found in porphyritic rocks having a microcrystalline groundmass which is composed mainly of more or less euhedral, tabular, or prismatic crystals.

H. Vesicular Structures

Scoriaceous: A highly vesicular structure similar to cinder. Gas cavities are numerous and roughly equidimensional, separated by thin walls of glass or aphanitic material.

Pumiceous: A rock froth, excessively cellular and usually having very thin glass walls separating the gas bubbles.

Amygdaloidal: Rocks in which gas cavities have subsequently been filled with introduced mineral material.

Miarolitic: Small angular gas cavities in phaneritic rocks into which crystals of the rock-forming minerals project.

I. Other Textural Features

Cataclastic textures: Textures developed by the mechanical crushing of rock or mineral grains.

Corona structure or reaction rim: A zone of one mineral surrounding another. The rim may be complete or partial.

Dendritic: Said of a mineral that has crystallized in a branching pattern.

Fluidal textures: An alignment of elements of the rock as a result of liquid flow.

Fusiform: Shaped like a spindle, i.e., tapering toward each end from a swollen middle.

Intergranular: Said of the ophitic texture of an igneous rock in which the augite occurs as an aggregation of grains, not in optical continuity.

Mesostasis: The last formed interstitial material, either glassy or aphanitic, of an igneous rock.

Ophitic: Said of the holocrystalline, hypidiomorphic-granular texture of an igneous rock (especially diabase) in which lath-shaped plagioclase crystals are partially or completely included in pyroxene crystals, typically augite. *Subophitic* implies partial inclusion.

Poikilitic: The texture of an igneous rock in which small grains of one mineral are irregularly scattered without common orientation in a typically anhedral larger crystal of another mineral.

Protoclastic: Said of igneous rocks in which the earlier formed crystals have been broken or deformed due to differential flow of the magma before complete solidification.

Symplectic: Said of a rock texture produced by the intimate intergrowth of two different minerals.

Trachytic: A textural term applied to volcanic rocks in which feldspar microlites of the groundmass have a subparallel arrangement corresponding to the flow lines of the lava from which they were formed.

J. Miscellaneous

Diabase/dolerite: An intrusive igneous rock whose main components are labradorite and pyroxene and which is characterized by ophitic texture.

Hypermelanic: An igneous rock that contains 90%-100% mafic minerals.

Mesotype: A group of zeolite minerals.

2. Metamorphic Terms

A. Mineral Form

Idioblastic: A crystal of metamorphic origin bounded by its own faces.

Xenoblastic: A crystal of metamorphic origin not bounded by its own faces.

B. Mineral Shapes

- Prismatic:** One dimension is markedly greater than the other two, forming a prism with or without terminations. Dimensions are on the order of a:b:3-5c.
- Acicular:** Slender needlelike crystals with or without visible crystal faces. Dimensions are usually a:b:10-20c, where a and b are a fraction of a millimeter.
- Bladed:** Three distinctly different dimensions, one of which is usually much larger than the other two. Dimensions are usually a:2-3b:5-10c.
- Tabular:** Two dimensions are markedly greater than the third; the crystal is usually bounded by two flat parallel faces and therefore has a uniform thickness. Dimensions are usually 3-10a:3-10b:c, with a and b either equal or nearly equal.
- Lenticular:** A lens-shaped crystal, thickest in the middle and tapering at the edges, often to a very thin edge. Dimensions are usually 2-5a:2-5b:c.
- Equant or equidimensional:** All three dimensions are equal or subequal but the crystal has an irregular shape.
- Blocky crystals:** All three dimensions are equal or subequal but the crystal has roughly planar sides.
- Spherical:** Equidimensional grains which have rounded boundaries.

C. Metamorphic Textures

- Crystalloblastic:** A crystalline texture produced by metamorphic recrystallization.
- Homeoblastic:** Essential mineral constituents are approximately the same size.
- Granoblastic:** A nonschistose rock with equidimensional crystals.
- Nematoblastic:** Development during recrystallization of slender parallel prismatic crystals.
- Lepidoblastic:** Foliated or schistose rock due to the parallel orientation during recrystallization of minerals with a flaky or scaly habit.
- Porphyroblastic:** A crystalloblastic texture with two or more distinct grain sizes. The individual large crystals are called porphyroblasts.
- Poikiloblastic:** A texture in which large porphyroblasts include numerous small crystal grains.
- Mosaic:** Crystals are equigranular and equidimensional and are generally polygonal in shape, with simple straight-line or

- gently curved intergranular boundaries.
- Sutured:** Crystals are generally equigranular and equidimensional, or they are lenticular and have highly irregular boundaries and much interpenetration of each grain into its neighbors.
- Cataclastic:** Textures produced by mechanical crushing without essential recrystallization.
- Mortar:** A texture consisting of larger mineral fragments set in a groundmass of crushed material derived from the same crystals.
- Mylonitic:** A very-fine-grained product of mechanical crushing without recrystallization of the primary minerals.
- Porphyroclastic:** A cataclastic texture characterized by the presence of large relict mineral grains set in a matrix of smaller crushed grains.
- Blasto-porphyratic:** Said of a relict texture in a metamorphic rock in which traces of an original porphyritic texture remain.

D. Foliation

Foliation is the general term used to include all planar textures and structures of metamorphic rocks which were developed during metamorphism. The foliation may be defined by layering of contrasting mineralogies (gneissosity), by planar preferred orientations of individual grains (schistosity), by planar fracture surfaces (cleavage), or by any combination of these three.

E. Lineation

A general term for the parallel orientation of textural or structural features that are linear.

BIOSTRATIGRAPHY

During the cruise, age determination was based on the study of each core-catcher assemblage. Nannofossils, planktonic foraminifers, and a paleoclimatic approach to the foraminiferal assemblages were used.

Age determinations were based on the following time scales (Fig. 12). Nannofossil zones used were the standard zonation of Martini (1971), with a change concerning the determination of the Pliocene-Pleistocene boundary using the extinction level of *Cyclcoccolithus macintyreii*.

For the Pleistocene we used the planktonic foraminifers biostratigraphic scale proposed by Ruggieri and Sprovieri (1983). Following the indication from the Pliocene-Pleistocene stratotype boundary section (Vrica section, Calabria, Italy), the base of the Pleistocene was recognized by the first strong increase of left-coiling *Neogloboquadrina pachyderma*. *Globigerina cariacensis* is always rare and scattered, and appears above this level. Paleomagnetic data, when available, are consistent with the so-identified boundary. It is here recognized that the *Globigerinoides obliquus*' last occurrence (l.o.) (the biostratigraphic event used on board to recognize the Pliocene/Pleistocene boundary) occurs above the base of the Pleistocene. These criteria are used in all the sites discussed in this report.

Pleistocene	<i>Emiliana huxleyi</i> NN21	<i>Globorotalia truncatulinoides</i> <i>excelsa</i> Total Range Zone	<i>Globorotalia truncatulinoides excelsa</i> f.o.
	<i>Gephyrocapsa oceanica</i> NN20		
	<i>Pseudoemiliana lacunosa</i> NN19		
late Pliocene	<i>Discoaster brouweri</i> NN18	MPI6 <i>Globorotalia inflata</i> Interval Zone	Strong increase in left-coiling <i>Neogloboquadrina</i> <i>Globorotalia inflata</i> f.o.
	<i>Discoaster pentaradiatus</i> <i>Discoaster surculus</i> NN17-NN16	MPI5 <i>Globigerinoides elongatus</i> Interval Zone	 <i>Sphaeroidinellopsis</i> l.o.
	<i>Reticulofenestra pseudoumbilica</i> NN15	MPI4 <i>Sphaeroidinellopsis subdehiscens</i> Interval Zone	 <i>Globorotalia margaritae</i> l.o.
	<i>Discoaster asymmetricus</i> NN14	MPI3 <i>Globorotalia margaritae-puncticulata</i> Concurrent Range Zone	 <i>Globorotalia puncticulata</i> f.o.
early Pliocene	<i>Ceratolithus rugosus</i> NN13	MPI2 <i>Globorotalia margaritae</i> Interval Zone	<i>Globorotalia margaritae</i> f.o.
	<i>Amaurolithus delicatus</i> NN12		
	MPI1 <i>Sphaeroidinellopsis</i> Interval Zone		
Messinian	<i>Discoaster quinqueramus</i> NN11b	Non - Distinctive Zone	Beginning of permanent open marine conditions. <i>Globigerina multiloba</i>
		<i>Globorotalia conomiozea</i> Interval Zone	 <i>Globorotalia conomiozea</i> f.o.
Tortonian	<i>Discoaster quinqueramus</i> NN11a	<i>Globorotalia suterae</i> Interval Zone	 <i>Globorotalia suterae</i> f.o.

Figure 12. Nannoplankton zones (Martini, 1971) and planktonic foraminiferal biostratigraphic scheme.

The biostratigraphic scale proposed by Cita (1975) and by Rio et al. (1984) was used for the Pliocene. Some zonal markers are rare and scattered near their first occurrence (f.o.) or l.o. levels, and only detailed studies of closely spaced samples make it possible to recognize these biostratigraphic events. This explains the difference between the results obtained on board, where only core-catcher samples were studied, and the results reported here, based on the study of several samples along the whole sequence.

For the Miocene the biozonation proposed by D'Onofrio et al. (1975) was used. This scale was completed, for the "evaporitic" Messinian interval, by the "non defined zone" described by Iaccarino (1985).

Our paleoclimatic approach was based on the curves of Glaçon (1985).

Foraminifer Abundance and Preservation

The abundance of foraminifers contained in sediment samples studied is defined as follows:

- A = abundant (about 2 cm³ of dry foraminifer residue from a 10-cm³ sample);
- C = common (about 1 cm³);
- F = few (about 0.5 cm³);
- R = rare (0.5 cm³ or less).

The abundance of particular species in the assemblages in a residue is defined as follows:

- A = over 30% of the population;
- C = 10%–30%;
- F = 3%–10%;
- R = less than 3%.

Percentages were estimated by visual examination.

Preservation includes the effects of diagenesis, epigenesis, abrasion, encrustation, and/or (most frequently in deep-sea sediments) dissolution.

- G = good (dissolution effects rare and obscure);
- M = moderate (specimen dissolution common but minor);
- P = poor (specimen identification very difficult or impossible).

Nannofossil Abundance and Preservation

Smear slides were prepared from raw sediment for examination of calcareous nannofossils. The abundance of nannofossils was estimated as follows:

- A = abundant (1–10 species per field of view);
- C = common (1 specimens per 2–10 fields of view);
- F = few (1 specimen per 11–100 fields of view);
- R = rare (1 specimen per 101–1000 fields of view).

This system was proposed by Hay (1970) using a magnification of 1000x; a magnification of 1560x was used in this study.

The state of preservation of nannofossils was designated as follows:

- G = little or no evidence of overgrowth and/or etching of specimen;
- M = some degree of overgrowth and/or etching, but identification generally not impaired;
- P = substantial overgrowth and/or etching, identification of specimens is difficult but still possible.

PALEOMAGNETISM

Leg 107 had an on-board three-axis cryogenic magnetometer (built by 2G Enterprises) capable of measuring both whole-round sections of cores and discrete samples. A three-axis alternating field (AF) demagnetization unit is mounted along the track. The entire operation, including multiple-step AF demagnetization, is under direct control of a DEC PRO-350 minicomputer. This magnetometer has great potential for obtaining detailed magnetostratigraphy from cores: it is possible to process a 9-m core using 5-cm spacing between measurements and three demagnetization steps and to obtain the final plot of declination and inclination within 2 hr, implying that the magnetostratigraphy and intensity variations can be determined before the core has been split for visual observation and sampling. However, in practice, several obstacles severely limited the use of this cryogenic magnetometer for routine whole-round analysis of cores on Leg 107.

The electronics for the magnetometer failed to arrive in Malaga before the departure of the ship. The electronics joined the ship in mid-cruise, but the cryogenic magnetometer was of limited use during this leg due to the high-coercivity/high-inclination overprint which affected most of the cores. The maximum peak AF available for whole-core treatment (80 Oe) was insufficient to remove this overprint. For this reason, most of the on-board measurements were done with the Molspin fluxgate magnetometer after AF treatments with the Schonstedt AF demagnetizer (GSD-1). Whole-core susceptibility measurements for some sites were carried out mainly using the Bartington susceptibility bridge.

Discrete samples were obtained from every section containing undisturbed sediments or basement rocks. In very soft material, oriented samples were taken by pressing plastic boxes (7-cm³ internal volume) into the sediment with one set of the sides maintained parallel to the axis of the core. In some semi-indurated sediments, an oriented cube was cut out of the section using a non-metallic knife and/or double-bladed diamond saw. One of the sampling techniques was to drill oriented minicores (2.4 cm diameter, 2.0–2.5 cm length) in the semi-indurated to lithified sediments and basement rocks. These were inscribed with an arrow parallel to the axis of the core. In sediments having a dip, the direction of dip relative to the axis of the minicore was recorded; these dip directions provide a relative coordinate system for declination control on the paleomagnetic samples.

The magnetic polarity time scale, which we use for reference, is that compiled by Harland et al. (1982). This scale is based on the Mankinen and Dalrymple (1979) compilation of radiometric age determinations from land sections for the Brunhes, Matuyama, and Gauss epochs, and on oceanic anomaly data for the Gilbert epoch which uses the 3.40 m.y. date for the age of the base of the Gauss and a constant seafloor-spreading model.

GEOCHEMISTRY

Carbonate and Organic Carbon Determinations

Shipboard organic carbon determinations were performed using a Perkin-Elmer 240C Elemental Analyzer to measure total carbon on ground and homogenized samples of 20 cm³. Approximately 40–50 mg of these samples was weighed with a Cahn 29 Automatic Electrobalance, which averages a total of 50 weight measurements to compensate for ship heave. Combusted at 1000°C in an oxygen atmosphere, concentrations of evolving CO₂ were determined against known standards and reported by the attached data station after background and blank corrections. Drift in the nitrogen detecting system and high blank values precluded the use of nitrogen concentrations and C/N ratios for

maturity and source determinations in most samples. Only safe and reliable values are reported in the tables. Carbonate carbon concentrations obtained from determinations with the Coulometrics Carbon Dioxide Coulometer Model 5010 were subtracted from total carbon to yield organic carbon. In the Coulometer, which has several distinct advantages over the carbonate bomb, 10–20 mg of the sample are digested in 2 mL 2N HCl. The gas is carried into a coulometric cell where it reacts with ethanolamine and causes the indicator to fade. The change in absorption is monitored by a photocell: a base is created electrically by the titration circuit until the solution returned to its original color. Frequent blank and standard runs show that this method for carbonate-carbon determination has a relative error of less than 1%, giving reliable values for subtraction of carbonate-carbon from total carbon to compute organic carbon. Standard runs and replicate analyses of standards of variable composition and C_{org} range show that this method has a relative error of less than 5% in sediments with C_{org} concentrations above 0.3%, and approximately 10% in organic carbon-lean sediments of less than 0.3% C_{org} .

Gas Analyses

Hydrocarbon gases, C_1 through C_5 , were monitored on a Hewlett-Packard (HP) 5890A Gas Chromatograph (GC) using a flame ionization detector. Methane levels were generally low, thus allowing good separation between methane and gases of higher molecular weight on a DC200 packed column. Run time for the analysis was 9 min. Methane, ethane, propane, *i*-butane, *n*-butane, *i*-pentane, and *n*-pentane separated in order of increasing retention time. Peak areas were measured and calibrated on a HP3392A Integrator and an HP3350 Laboratory Automation System (LAS).

Samples were collected through the core liner in vacutainers, and a 10-cm³ sediment sample, used for headspace analysis, was collected upon initial sectioning of the core. The sediment sample was placed in a 20-cm³ glass vial and sealed immediately with a septum and crimped metal cap. The vial was then heated in a hot oil bath at 70°C for 1 hr. The oil bath was part of the HP19395A Headspace Sampler (HSS). After equilibration, the HSS performs a preprogrammed sequence using an automated valve and loop sampling system. A sampling needle pierces the septum, and helium pressurizes the headspace vial. The headspace gas is vented to the GC through a 0.25-mL sample loop. The loop is then flushed into the helium carrier gas flow, and the sample is delivered through a heated transfer line directly into the GC's injection port.

Vacutainer samples were delivered to the GC through the HSS. A 5-mL syringed sample was injected into a manual injection port on the HSS which filled the 0.25-mL sample loop. The HSS then injected the sample to the GC as previously described.

Concentrations of hydrocarbon gases were computed from detector responses of canned gas standards, and preprogrammed methods were set up in the LAS to cover a wide range of concentrations.

Bitumen Extraction and Gas Chromatography

Selected samples were subjected to solvent extraction of bitumen to tentatively characterize origin and maturity of organic matter.

Several grams of samples were dried, ground, weighed, and subjected to ultrasonic waves for 2 hr with a mixture of methanol/toluene (3:1). After centrifuging and decanting the solvent containing total extractable hydrocarbons, the extract was evaporated to dryness and weighed. In most cases, the small amount of sample and of the resulting extract precluded quantification. Redissolved in HPLC-grade *n*-hexane, non-aromatic hydrocarbons were separated from aromatic and NSO components by

liquid chromatography on commercial CN and silica gel columns (Baker 10, provided in the lab). The hexane eluent from these columns was again evaporated and redissolved in 1 mL of hexane. Of these purified extracts, 2–4 μ L were injected into a 5890A GC equipped with a 25-m high-performance capillary. Instrument setup and column characteristics are given below.

The Hewlett Packard 5890A gas chromatograph was used with the following experimental condition:

1. Temperature program: Injection at 200°C, Flame ionization detector (FID) 300°C; Initial temperature (1 min) 40°C, Rate A 50°C/min to 80°C, Purge on after 0.8 min, 1 min at 80°C, Rate B 10°C/min to 300°C, 300°C for 5 min.

2. Column: 25-m high-performance capillary, cross-linked methyl silicone, internal diameter 0.2 mm, film thickness 0.11 μ m, splitless injection.

Retention times from a *n*-alkane standard were used to identify saturated acyclic components. Runs were reported through the HP LAS and plotted with the CPlot routine. Ratios of components were computed after manual background correction and automated integration of peaks.

Interstitial Waters

Interstitial waters were routinely analyzed for pH, alkalinity, salinity, chlorinity, calcium, and magnesium during Leg 107. The method of obtaining interstitial waters from the sediment, using a stainless steel press, has been described in detail by Manheim and Sayles (1974). IAPSO (International Association of Physical Science Organizations) standard seawater is the primary standard for water analyses on board ship.

Alkalinity and pH were determined using a Metrohm titrator with a Brinkmann combination pH electrode. The pH value of the sample was calibrated with 4.01, 6.86, and 7.41 buffer standards; readings were taken in millivolts and then converted to pH. The pH measurements were made immediately prior to the alkalinity measurements. The 5–10 mL interstitial water sample, after being tested for pH, was titrated with 0.1 N HCl as a potentiometric titration.

Salinity was determined using a Goldberg optical refractometer which measures the total dissolved solids.

Chlorinity was determined by titrating a 0.1-mL sample diluted with 5 mL of deionized water with silver nitrate. The Mohr titration uses potassium chromate as an indicator.

Calcium was determined by complexometric titration of a 0.5-mL sample with EGTA using GHA as an indicator. To enhance the determination of the end point, the calcium-GHA complex was extracted into a layer of butanol. No correction was made for strontium, which is also included in the result.

Magnesium is determined by EDTA titration for total alkaline earths. Subsequent subtraction of the calcium value (also includes strontium) yields the magnesium concentration in the interstitial water sample.

For determinations of Ca^{2+} , Mg^{2+} , and SO_4^{2-} by ion chromatography a 0.2/100 dilution of the samples was prepared with deionized water. The samples were analyzed on the Dionex Ion Chromatograph which is equipped with both anion and cation separation columns. The samples are compared to a series of standards containing concentrations of species varying from 0 to 61.4 mmol/L (SO_4^{2-} and Mg^{2+}) and from 7.24 to 43.7 mmol/L (Ca^{2+}) by a curve-fitting routine on the HP-97 calculator. Samples and standards are run in triplicate, and a water blank is run after each set of three to decrease the carry-over from set to set.

Comparisons of Ca^{2+} and Mg^{2+} methods by Gieskes and Peretsman (1986) show that results obtained by titration and ion chromatography agreed well. We found the same agreement in samples of Hole 650 and 651 for both methods.

PHYSICAL PROPERTIES PROCEDURES

A thorough discussion of physical properties is presented by Boyce (1973, 1976) with respect to equipment, methods, errors, correction factors, and problems related to coring disturbance. Only a brief review of methods employed on Leg 107 is given here.

GRAPE

The Gamma Ray Attenuation Porosity Evaluator (GRAPE), described in detail by Boyce (1976), was used to continuously measure the wet-bulk density of material in core sections over 50 cm long. Where indurated rock samples did not completely fill the core liner, the diameter of the rock pieces was individually measured with a caliper and the data entered in a specially designated column on the shipboard visual core descriptions alongside the graphic representation of the measured piece.

Thermal Conductivity

Thermal-conductivity measurements were made on undisturbed sediments from cores which recovered material soft enough to yield to needle-probe insertion. Data were collected by inserting needle probes through small (about 1-mm diameter) holes drilled in the core liners. These probes are connected to a Thermcon-85 unit (Koehler and Von Herzen, 1986) mated to a PRO-350 computer system. The software computes the coefficient of conductivity as a function of changes in resistance in the needles induced by changes in temperature over a 6-min interval. One probe is inserted in a rubber standard and run with each set of measurements. Drift must be less than $4 \times 10^{-2} \text{C/min}$ for reliable data. This accuracy requires allowing cores to thermally equilibrate to room temperature for at least 3 hr prior to determining conductivity. Temperature drift was generally less than 0.04C/min at the time of thermal conductivity measurement.

Vane Shear

A complete discussion of the vane shear apparatus and shear strength measurement appears in Boyce (1973). Undrained shear strength was measured by a Wykeham Farrance vane shear rotating at $89^\circ/\text{min}$. Measurements of vane shear strength were routinely made on sediments with shear strengths less than about 70 kP (i.e., until the sediment was of sufficient cohesive strength to form drilling "biscuits"). Measurement were made perpendicular to the split core face for each interval sampled.

Velocity

Compressional sound velocity at 500 kHz was measured through sediments, sedimentary rocks, and igneous rocks with a Hamilton Frame Velocimeter using a Tektronix 5110 oscilloscope and Tektronix TM5006 Counter/Timer. Sound velocity correction factors were calculated for each hole on Leg 107 as described in Boyce (1976).

Index Properties

Index properties (bulk density, grain density, and porosity) were routinely measured gravimetrically on the same samples for which seismic velocity was measured. Samples were placed in pre-weighed and numbered aluminum beakers and weighed in the beakers on a Kahn 29 Automatic Electrobalance which averages 50 weight measurements to compensate for ship heave. The volume of sample and container was then measured on the shipboard Penta-Pycnometer, which first purges the sample chamber of air, and then floods the sample chambers with helium gas at a pressure of 1.34 kg/cm^2 . The volume of sample and container is calculated from the difference between volume of helium in the empty sample chamber and in the chamber with sample. Samples were dried at 104°C for 24 hr, then freeze-dried for 24 hr, weighed and their dry volume measured. Index

properties were calculated by a computer program in which sample container and volume had been previously entered.

The pycnometer and electric balance used on board to compute grain density, bulk density and porosity have a precision of $\pm 0.05 \text{ cm}^3$ and $\pm 0.02 \text{ g}$. As a consequence, the measurements performed on board allowed a precision of grain density, bulk density, and porosity of about 1% for unconsolidated sediments and about 2% for consolidated sediments and hard rocks.

Small basalt samples ($3\text{--}5 \text{ cm}^3$) were used to compute their physical properties; because of the high vesicularity of the basalts recovered during Leg 107, it was not possible to saturate those samples on board. However, porosity of vesicular basalt was calculated, but the results were interpreted emphasizing the trends of the average values rather than the absolute values.

Salinity-corrected physical properties were computed for all split core samples assuming a pore water salinity of 35%.

After measurement of sample dry weight and dry volume, the carbonate content of the samples was measured using the CO_2 coulometer method.

DOWNHOLE MEASUREMENTS

Logs

Eight logging probes were used during Leg 107 (Table 1). The tools were developed by Schlumberger for oil-field applications, and in some cases were modified for use aboard the ship by ODP. Three or four tools are stacked atop one another (Fig. 13) and lowered in three logging runs.

RUN 1—Resistivity-Sonic Velocity-Gamma Ray-Caliper

Electrical resistivity (DIL). The dual induction log provides three different measurements of electrical resistivity, each one with a different depth of investigation. Two induction devices (deep and medium resistivity) employ an array of coils operating at 25 kHz. The high frequency alternating currents sent through the transmitter coils create magnetic fields which induce secondary (Foucault) currents in the formation (Fig. 14). These ground-loop currents produce new inductive signals, proportional to the conductivity of the formation, which are recorded by the receiving coils. The depth of penetration of the measurements is influenced by the spacing between transmitting and receiving coils. A third device (spherically focused resistivity) measures the current necessary to maintain a constant voltage drop across a fixed interval, at near-DC frequencies. The medium and deep resistivity devices provide a vertical resolution of around 2 m, the focused resistivity of about 1 m.

Water content and salinity are by far the most important factors controlling the electrical resistivity of rocks. To first order, the resistivity responds to the inverse square root of porosity (Archie, 1942). Other factors influence resistivity, such as the concentration of hydrous and metallic minerals, vesicularity, and geometry of interconnected pore space.

Sonic velocity (LSS). The long-spacing sonic probe uses two acoustic transmitters spaced 2 ft (0.61 m) apart and two receivers also spaced 2 ft apart and located 8 ft (2.43 m) below the transmitters. The data are expressed as time required for a sound wave to travel through 1 ft (0.31 m) of formation (Fig. 15). Compensation for borehole irregularities and inclination of the tool to the hole axis is obtained by memorizing the first transit time reading and averaging it with a second reading obtained after the sonde has been pulled up by a fixed distance along the borehole. First arrivals for the individual source-receiver paths are used to calculate the velocities of the different waves traveling in the formation (compressional, shear, etc.). The vertical resolution of the tool is about 0.61 m.

Compressional-wave velocity is dominantly controlled by porosity and lithification; decreases in porosity and increases in lithification cause the velocity to increase. In crystalline rocks

Table 1. Summary of log measurements.

Mnemonic	Tool	Measurement	Unit
CALI	Caliper	Hole size	inches
GR	Natural Gamma Ray	Natural radioactivity	GAPI
DIL	Dual Induction	Deep, medium, and focused resistivity	m
LSS	Long Spacing Sonic	Sonic transit time (short and long spacing)	$\mu\text{s}/\text{ft}$
LDT	Lithodensity	Bulk density	g/cm^3
CNT	Compensated Neutron	Photoelectric effect	barns/e-%
NGT	Natural Gamma Spectrometry	Porosity	%
		Total (Th + U + K) and computed (Th + K) natural radioactivity	GAPI
		Uranium, thorium	ppm
		Potassium	weight %
GST	Induced Gamma Spectrometry	Elemental yields (Ca, Cl, H, Fe, S, Si)	

such as those logged at Site 655 the pore shape distribution also influences the measured velocities. Flat or ellipsoidal pores or cracks cause a larger velocity diminution than an equal volume of rounded or subrounded pores. In both crystalline and sedimentary rocks, attenuation of the different arrivals (as seen on the waveforms themselves) is controlled by mechanical property changes.

Caliper (CALI). A three-arm caliper measures the borehole size as a function of depth. Such a measurement is often required to correct logs whose response is affected by the borehole diameter.

Natural gamma ray (GR). The Gamma Ray tool measures the natural radioactivity of the formation. Most gamma rays are emitted by the radioactive isotope K^{40} and by the radioactive elements of the U and Th series. Passing through the material, gamma rays are scattered through collisions with the atoms of the formation, losing energy until they are absorbed. The gamma ray radiation originating in the formation close to the borehole wall is measured by a scintillation detector mounted inside the sonde. The average formation depth of investigation is about 0.31 m.

Since radioactive minerals tend to concentrate in clays and shales, the gamma ray curve is often used to estimate the clay or shale content. There are rock matrices, however, whose radioactivity ranges from moderate to very high values, due to the presence of volcanic ash, potassic feldspar, or other radioactive minerals.

RUN 2—Lithodensity-Neutron Porosity-Natural Spectral Gamma Ray

Lithodensity tool (LDT). This tool utilizes a Ce^{137} gamma ray source to measure the resulting flux at fixed distances from the source. Under the operating conditions, attenuation of gamma rays is chiefly due to Compton scattering (Dewen, 1983); thus the resultant count rates can be related to the formation bulk density. The radioactive source and detector array is placed in a skid which is pressed against the borehole wall by a strong spring (Fig. 16). Excessive roughness of the hole will cause some drilling fluid to infiltrate between the skid and the formation. As a consequence, density readings will be artificially low. Corrections can be applied by using caliper data.

In addition to bulk density, a photoelectric effect index is also provided. Photoelectric absorption occurs in the energy window below 150 keV and depends on the energy of the incident gamma ray, the atomic cross section, and the nature of the atom. Since this measurement is almost independent of porosity, it can be used directly as a matrix lithology indicator.

The depth of investigation of the lithodensity tool depends on the density of the rock—the higher the density, the lower the penetration. In porous and permeable formations the density

tool does not read deeper than 0.15 m into the formation. The vertical resolution is about 0.30 m.

Compensated neutron porosity (CNT). A radioactive source mounted on the sonde emits fast neutrons (5 MeV) into the formation, where they are scattered and slowed by collisions with other nuclei. When the neutrons reach a low energy level (0.025 MeV) they are captured and absorbed by atomic nuclei such as hydrogen, chlorine, silicon, and boron. The scattering cross section is the quantity that describes the rate at which neutrons are slowed. Since the scattering cross section for hydrogen is about 100 times larger than for any other common element in the crust, most energy dissipation is caused by collisions with water molecules. Therefore, a change in the number of neutrons detected at a receiver can be related inversely to porosity. In practice, an array of detectors is used to minimize borehole or drilling fluid effects. As with the LDT, the tool should be held in contact with the formation. Porosity measurements made in presence of hydrous minerals will be overestimates of the true porosity. The vertical resolution of the tool is about 0.25 m.

Natural spectral gamma ray (NGT). This tool measures the three different components (K, Th, and U) of the spectrum of the detected gamma rays, differentiating between gamma rays of different energies. The sonde consists of a sodium iodide detector contained in a pressure housing; a downhole electronic amplifier transmits pulses through the logging cable to the surface panels including a multichannel analyzer which displays the entire spectrum and selects pulses within preselected energy windows. The abundances of the individual radioactive elements are often distinctive markers. Volcanogenic sediments recovered at Site 651 (see Site Chapter, this volume), for example, display unusually high concentrations of uranium and thorium.

The investigation depth of the tool depends on hole size, mud and formation density, and on the energy of gamma rays. Higher energy radiation can reach the detector from deeper in the formation.

RUN 3—Induced Spectral Gamma Ray-Neutron Porosity-Natural Spectral Gamma Ray

Induced spectral gamma ray (GST). The tool consists of a pulsed source of 14-MeV neutrons and a gamma ray scintillation detector. A surface computer performs spectral analysis of gamma rays resulting from the interactions of neutrons emitted by the source with atomic nuclei in the formation. Several elements can be characterized by typical sets of gamma rays emitted through given neutron interactions. At each depth the computer determines a weighed least square estimate of the combination of standard spectra which best fits the logged gamma ray spectrum (Hertzog, 1979).

Six elemental yields, (i.e., the contribution to the total spectrum), are calculated: Ca, Si, Fe, Cl, H, and S. As their sum is

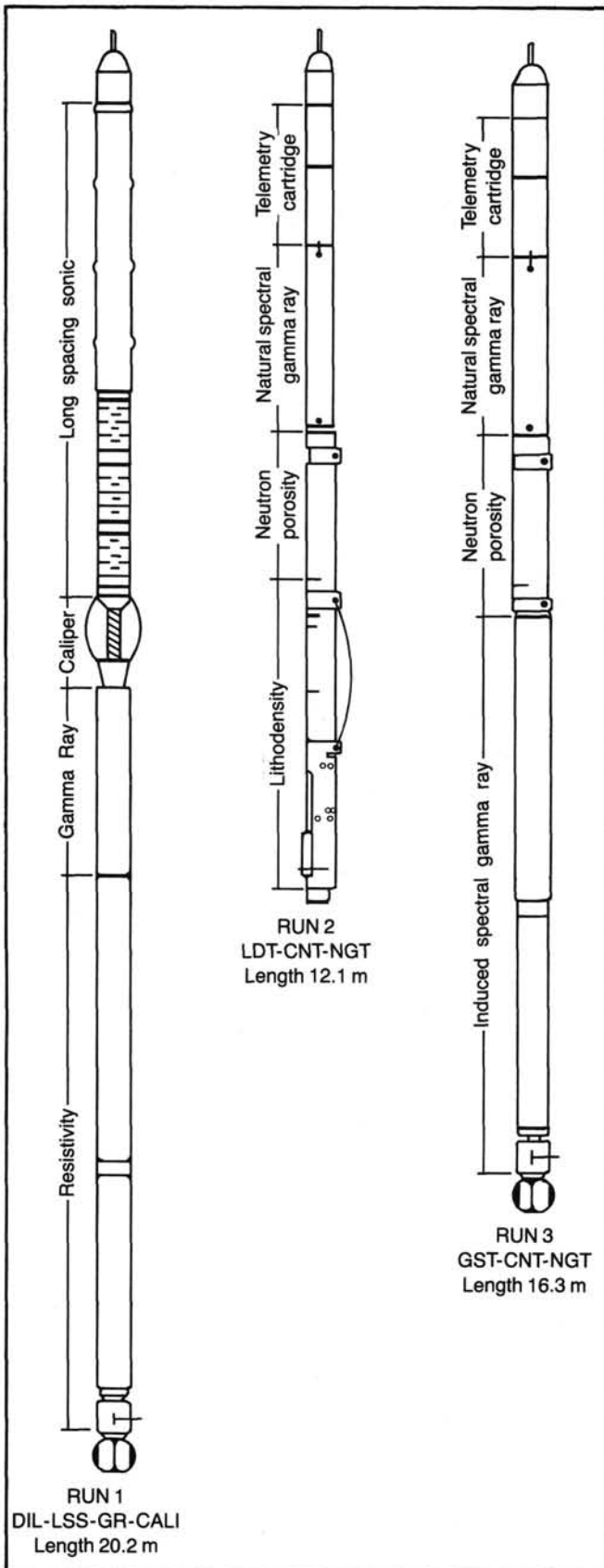


Figure 13. Schematic diagram showing the combinations of logging tools run during Leg 107.

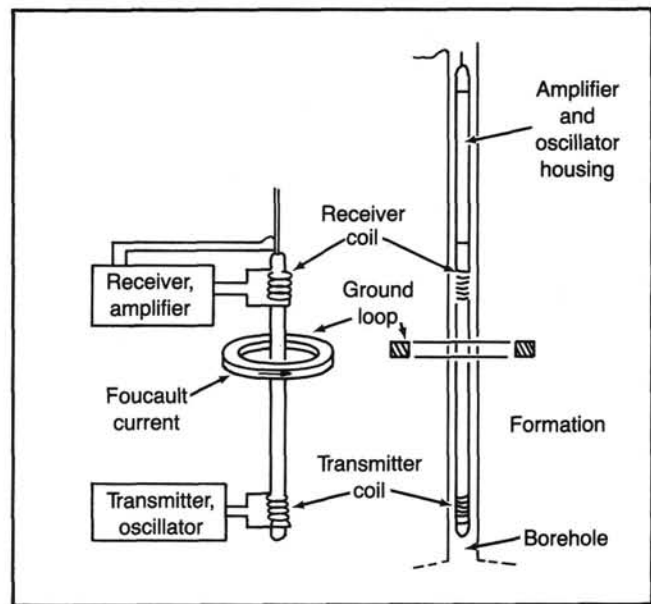


Figure 14. Basic two-coil induction log system (DIL) from Schlumberger (1972).

always one, they do not reflect the actual elemental composition. Therefore, ratios of these yields must be used in the interpretation of lithology, porosity, and salinity of the formation fluid.

The GST can be run through the drill pipe and in cased holes, thus it can be used in holes which otherwise could not be logged due to bad hole conditions. The GST is run in combination with the natural gamma spectrometry and neutron porosity tools. It is not run along with the lithodensity tool because both tools are designed to be located at the bottom of the tool string.

A summary of logging tools run during leg 107 and their specifications are shown in Tables 1 and 2. A detailed description of logging tool functioning and of their applications is provided in Dewen (1983), Hertzog (1979), Schlumberger (1972), Serra (1984), and Timur and Toksoz (1985).

Log Data Quality

Log data quality may be seriously degraded in excessively large sections of the borehole or by rapid changes in the hole diameter. Resistivity and velocity measurements are less sensitive to borehole effects, while the nuclear measurements (neutron porosity and natural and induced spectral gamma ray) are most seriously impaired, because of the large attenuation by the borehole fluid. Corrections can be applied to the original data in order to reduce the effects of these conditions and, generally, any departure from the conditions under which the tool was calibrated.

One of the most serious problems which affect all logging data is the depth mismatching between logs and cores, caused by ship heave during the recording. Small errors in depth matching can impair the results in zones of rapidly varying lithology. To minimize such errors, a hydraulic heave compensator adjusts for rig motion in real-time. Unfortunately, 100% accuracy is not obtainable in zones where core recovery is low because of the inherent ambiguity of placing the recovered section within the interval cored.

HEAT FLOW

Temperatures were obtained using two different types of equipment. During the Advanced Piston Coring (APC) penetration

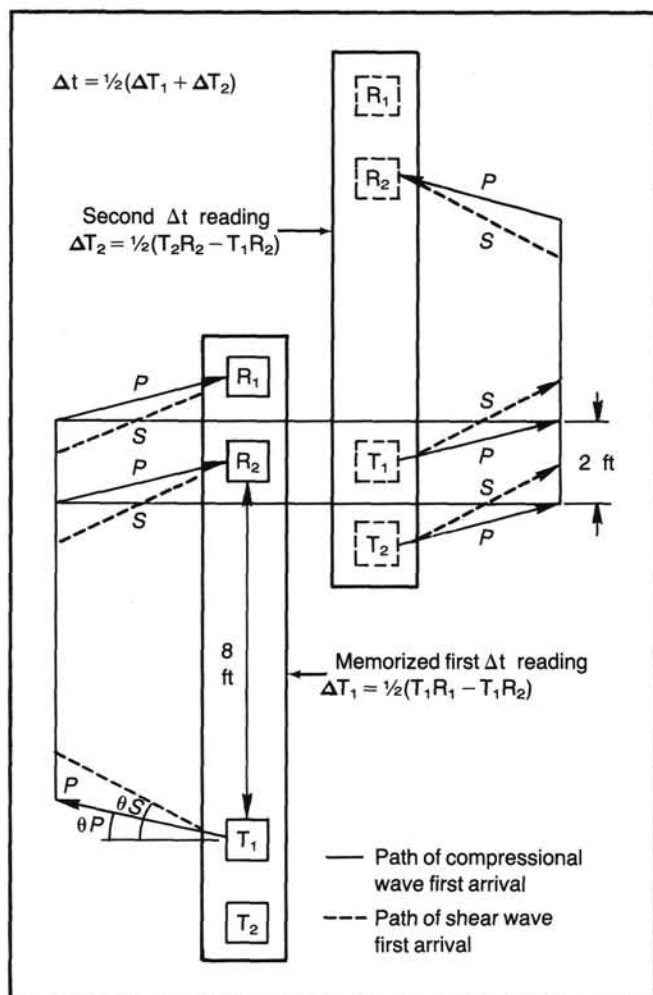


Figure 15. Long Spacing Sonic (LSS) configuration. The first transit time reading (ΔT_1) is memorized and then averaged with a second reading (ΔT_2) obtained after the sonde has been pulled up by a fixed distance along the borehole (after Schlumberger, 1982).

of the uppermost sedimentary series the Von Herzen temperature probe was used. The thermistor is located in a short and strong needle, at the base of the core barrel. This new probe utilizes integrated circuit memory units to record the downhole temperature. It is possible to digitally record variations of the thermistor resistance sampled every 15 s on digital cassette tape with high resolution into the self-contained T recorder. Stored data are read aboard the *JOIDES Resolution* through a computer program converting resistance into temperature, using the

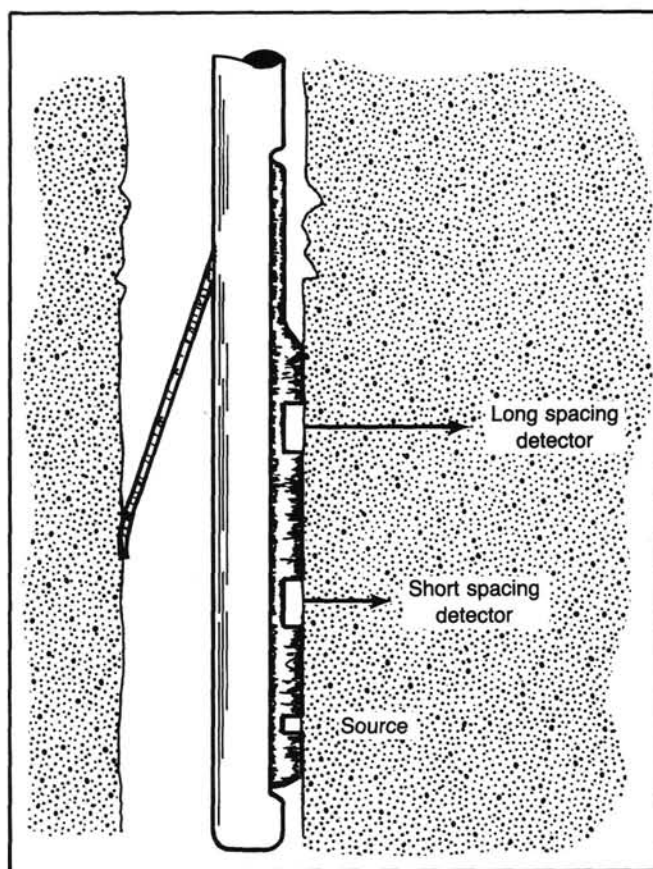


Figure 16. Dual spacing Lithodensity Tool (LDT) after Schlumberger (1972). Good quality readings are obtained when the detector skid is held in contact with the formation by a spring. Excessive roughness of the hole (upper part of the figure) will cause some drilling fluid to infiltrate between the skid and the formation and the readings to be artificially low.

thermistor calibration data. Temperature records are presented as a listed file of resistance-temperature vs. time. An automatic plotting routine traces the temperature curve vs. time making it possible to plot the curve of temperature measurement into the sediment (Fig. 17). Ideally this curve should show an abrupt frictional heating effect, slowly decreasing down to the equilibrium temperature after a few minutes. One of the most significant advantages of using the Von Herzen probe is that if the total equilibrium temperature is not obtained because penetration into the sediment is not maintained long enough, the temperature can be deduced from such a curve by extrapolation. The temperature can be estimated by extrapolating the recorded tem-

Table 2. Tool specifications.

Tool	Source	Transmitters	Receivers (detectors)	O.D. (in.)	Length (in.)	Weight (lbs)	Max. Temp. (°F)	Max. Press. (psi)
CALI	—	—	—	3 3/8	60	120	350	20,000
CNT	Am/Be ²⁴¹	—	4	3 3/8	153	213	350	20,000
GR	—	—	1	3 3/8	60	125	350	20,000
GST	*a	—	1	3 3/8	444	505	350	20,000
LDT	Ce ¹³⁷	—	2	3 3/8	245	381	350	20,000
LSS	Acoustic	2	2	3 3/8	309	441	350	20,000
NGT	—	—	1	3 3/8	100	165	300	20,000
DIL ^b	—	—	—	3 3/8	346	335	350	20,000

a * Accelerator tube containing ions of deuterium and tritium.
 b Dual induction log (resistivity) tool has nine electrodes.

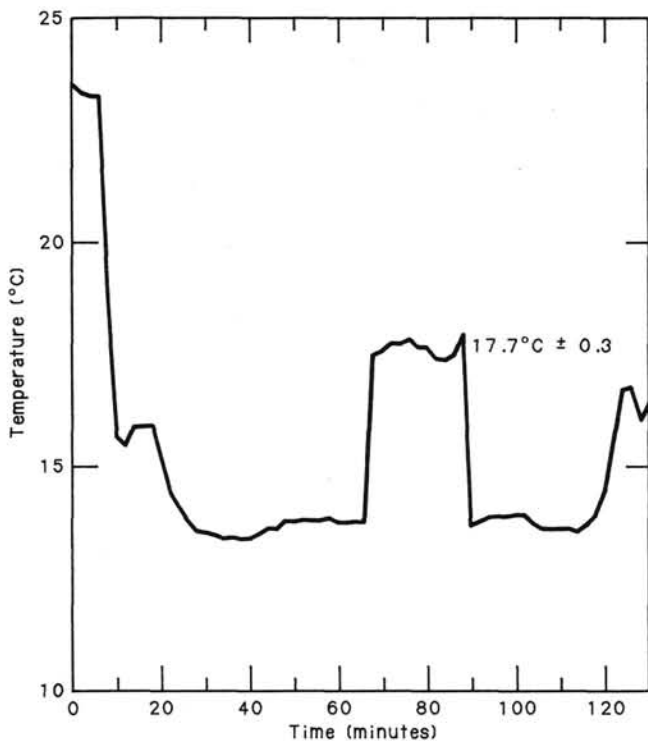


Figure 17. Downhole temperature measurements in Hole 651A at sub-bottom depth 29.4 m.

peratures from the first few minutes after penetration using an $F(\alpha, t)$ function to describe the frictional heating transient (Bullard, 1954). Even with the large size of the nose of the probe, a simple form of (α, t) , i.e., $T \propto 1/t$ is allowed.

During extended core barrel (XCB) drilling and during rotary drilling operations the Uyeda/Kinoshita temperature probe was used. In this procedure an entirely self-contained temperature recorder is inserted into a core barrel with a thermistor probe protruding about 30–50 cm through the center of the core catcher. After drilling to the depth where a temperature measurement was scheduled, the core barrel was lowered on the wire line to the bottom of the drill string. Once the core barrel was locked into the bottom-hole assembly, the drill string was gradually lowered to the bottom of the hole. Lowering pushed the thermistor probe into the undrilled sediment in front of the bit, where it remained for approximately 15–20 min. Resistance of the thermistor was measured every 0.5 s and put into integrated circuit memory at either 1-min or 2-min intervals. One hundred twenty-eight readings can be stored in the memory (which gives a 2-hr 8-min operating record at a sampling rate of 1 sample per minute). Data can be read out either automatically or manually.

Calm seas and an alert and skilled drilling team and lab technicians were major assets in the collection of high-quality data.

REFERENCES

- Archie, G. E., 1942. The electrical resistivity log as an aid in determining some reservoir characteristics. *Pet. Technol.*, 5(1).
- Bates, R. L., and Jackson, J. A., (Eds.), 1980. *Glossary of Geology*. Falls Church, VA (Am. Geol. Inst.).
- Boyce, R. E., 1973. Appendix I. Physical property methods. In Edgar, N. T., Saunders, J. B., et al., *Init. Repts. DSDP*, 15: Washington (U.S. Govt. Printing Office), 1115–1128.
- , 1976. Appendix I. Definitions and laboratory techniques of compressional sound velocity parameters and wet-water content, wet-bulk density, and porosity parameters by gravimetric and gamma ray attenuation techniques. In Schlanger, S. O., Jackson, E. D., et al., *Init. Repts. DSDP*, 33: Washington (U. S. Govt. Printing Office), 931–958.
- Bullard, E. C., 1954. The flow of heat through the floor of the Atlantic Ocean. *Proc. R. Soc. London, A*, 222:408–429.
- Cita, M. B., 1975. Studi sul Pliocene e gli strati di passaggio del Miocene al Pliocene, VIII. Planktonic foraminiferal biozonation of the Mediterranean deep sea record: a revision. *Riv. Ital. Paleontol. Stratigr.*, 81:527–544.
- Dewen, J. T., 1983. *Essentials of Modern Open Hole Log Interpretations*. Tulsa (Penwell).
- D'onofrio, S., Giannelli, L., Iaccarino, S., Morlotti, E., Romeo, M., Salvatorini, G., Sampo, M., and Sprovieri, R., 1975. Planktonic foraminifera of the Upper Miocene from some Italian sections and the problem of the lower boundary of the Messinian. *Boll. Soc. Paleontol. Ital.*, 14,2:177–196.
- DSDP, 1983. Design and operation of the hydraulic piston corer. *DSDP Tech. Rept. 12*.
- , 1984. Design and operation of an advanced hydraulic piston corer. *DSDP Tech. Rept. 21*.
- Gealy, J. M., Winterer, E. L., and Moberly, R. M., Jr., 1971. Methods, conventions, and general observations. In Winterer, E. L., Riedel, W. R., et al., *Init. Repts. DSDP*, 7, Pt. 1: Washington (U.S. Govt. Printing Office), 9–26.
- Gieskes, J. M., and Peretson, G., 1986. Water chemistry procedures aboard JOIDES Resolution: some comments. *ODP Tech. Note 5*.
- Glaçon, G., 1984. La marge et les fosses helléniques; campagnes Ariane et Egion du programme heat, In *Rapport des campagnes à la Mer, CNEXO*, 24:1–160.
- Harland, W. B., Cox, A. V., Llewellyn, P. G., Pickton, C.A.G., Smith, A. G., and Walters, R., 1982. *A Geologic Time Scale*. Cambridge (Cambridge Univ. Press).
- Hay, W. W., 1970. Cretaceous nannofossils from cores recovered on Leg 4. In Bader, R. G., Gerard, R. D., et al., *Init. Repts. DSDP*, 4: Washington (U.S. Govt. Printing Office), 455–501.
- Hertzog, R., 1979. Laboratory and field evaluation of an inelastic-neutron-scattering and capture gamma ray spectroscopy tool. *Soc. Pet. Eng. Pap.* 7430.
- Iaccarino, S., 1985. Mediterranean Miocene and Pliocene planktic foraminifera. In Bolla, H. M., Saunders, J. B., and Perch-Nielson, K., (Eds.), *Plankton Stratigraphy*: Cambridge (Cambridge Univ. Press).
- Jackson, K. C., 1970. *Textbook of Lithology*. New York (McGraw Hill).
- Koehler, R., and Von Herzen, R., 1986. A miniature deep sea temperature data recorder: Design, construction and use. *Woods Hole Oceanogr. Inst. Tech. Rept.* 86-3.
- Manheim, F. T., and Sayles, F. L., 1974. Composition and origin of interstitial waters of marine sediments based on deep sea drill cores. In Goldberg, E.D., (Ed.), *The Sea*, 5: New York (Wiley), 527–568.
- Mankinen, E. A., and Dalrymple, G. B., 1979. Revised geomagnetic polarity time scale for the interval 0–5 my B.P. *J. Geophys. Res.* 84: 615–626.
- Martini, E., 1971. Standard Tertiary and Quaternary calcareous nannoplankton zonation. In Farinacci, A. (Ed.) *Proc. Planktonic Conf. II Rome 1970*, Rome (Technoscienza), 2:739–785.
- Matthews, D. J., 1939. *Tables of Velocity of Sound in Pore Water and in Seawater*: London (Admiralty, Hydrogr. Dep.).
- Ocean Drilling Program, 1985. Shipboard scientist's handbook. *ODP Tech. Note 3*.
- Pelletier, G. L., and Von Herzen, R. P., 1985. THERMCON 85. Thermal conductivity instrument. *Instruction Manual For Use with DEC PRO-350*. May 85, ODP.
- Ratcliffe, E. H., 1960. The thermal conductivities of ocean sediments. *J. Geophys. Res.*, 65:1535–1541.
- Rio, D., Sprovieri, R., and Raffi, I., 1984. Calcareous plankton biostratigraphy and biochronology of the Pliocene-Lower Pleistocene succession of the Capo Rossello area, Sicily. *Mar. Micropaleontol.*, 9:135–180.
- Ruggieri, G., and Sprovieri, R., 1983. Recenti progressi nella stratigrafia del Pleistocene inferiore. *Boll. Soc. Paleontol. Ital.*, 22,3:315–321.
- Schlumberger, 1972. *Log Interpretation* (Vol. 1, Principles). New York (Schlumberger Ltd).
- Schmid, R., 1981. Descriptive nomenclature and clarification of pyroclastic deposits and fragments: recommendations of the IUGS Sub-commission on the Systematics of Igneous Rocks. *Geology*, 9:41–43.

SHIPBOARD SCIENTIFIC PARTY

- Serra, O., 1984. Detailed description of logging tool functioning and applications *In Developments in Petroleum Science*: Amsterdam (Elsevier).
- Steiner, M. B., 1977. Magnetization of Jurassic red deep-sea sediments in the Atlantic (DSDP Site 105). *Earth Planet. Sci. Lett.*, 35:205-214.
- Supko, P., Ross, D. A., and Neprochnov, Y. P., 1978. Introduction and explanatory notes, Leg 42B, Deep Sea Drilling Project. *In* Ross, D. A., Neprochnov, Y. P., et al., *Init. Repts. DSDP*, 42, Pt.2: Washington (U.S. Govt. Printing Office), 3-15.
- Timur, A., and Toksoz, M. N., 1985. Fundamentals of well log interpretation. *Ann. Rev. Earth Planet. Sci.*, 13:315-344.
- Tomkeieff, S. I., 1983. *Dictionary of Petrology*. New York (John Wiley).
- Von Herzen, R. P., and Maxwell, A. E., 1959. The measurement of thermal conductivity of deep sea sediments by a needle-probe method. *J. Geophys. Res.* 64:1557-1563.
- Wentworth, C. K., 1922. A scale of grade and class terms of clastic sediments. *J. Geol.*, 30:377-390.
- Wentworth, C. K., and Williams, H., 1932. The classification and terminology of the pyroclastic rocks. *Rept. Comm. Sedimentation, Bull. Nat. Res. Council. (U.S.)*, 80:10-53.
- Zoback, M. D., and Anderson, R. N., 1982. Ultrasonic borehole televiewer investigation of oceanic crustal layer 2A, Costa Rica Rift. *Nature*, 295:375-379.